Depositional history of Devonian to lower Carboniferous (Tournaisian) strata, northern Wyoming and southern Montana, USA

Mingxi Hu[1,2], Paul M. Myrow[1], David A. Fike[2], Mercedes di Pasquo[3], Michał Zatoń[4], Woodward W. Fischer[5], and Michael Coates[6]

[1]*Department of Geology, Colorado College, Colorado Springs, Colorado 80903, USA*
[2]*Department of Earth and Planetary Sciences, Washington University, St. Louis, Missouri 63130, USA*
[3]*Laboratory of Palynostratigraphy and Paleobotany, Centro de Investigación Científica y de Transferencia de Tecnologìa a la Producción, Consejo Nacional de Investigaciones Científicas y Técnicas, Gobierno de la Provincia de Entre Ríos, Universidad Autónoma de Entre Ríos, E3105BWA Diamante, Entre Ríos, Argentina*
[4]*Institute of Earth Sciences, University of Silesia in Katowice, Będzińska 60, 41-200 Sosnowiec, Poland*
[5]*Division of Geological and Planetary Sciences, California Institute of Technology, Pasadena, California 91125, USA*
[6]*Department of Organismal Biology and Anatomy, University of Chicago, Chicago, Illinois 60637, USA*

ABSTRACT

The lower Frasnian (Upper Devonian) Maywood Formation records incision of valleys into lower Paleozoic bedrock in fluvial to estuarine settings in northern Wyoming and deposition in estuarine to marine environments in southern Montana (USA). A distinctive fossil assemblage of microconchids, plant compression fossils, fish fossils, and microspores represent fauna and flora that lived in, and adjacent to, salinity-stressed ecological niches in the upper reaches of the Maywood valleys. A similar fossil assemblage is recorded in older Devonian valley-fill deposits of the Lower Devonian Beartooth Butte Formation, indicating that valley incision and subsequent transgression, occurred repeatedly over a span of nearly 30 million years with organisms tracking the marine incursions into the valleys. The fossil charcoal in the Maywood Formation captures a record of fire in adjacent terrestrial ecosystems. The amount of dioxygen (O_2) was thus above the fire window level (16% by volume) and might have been near modern levels in the earliest Late Devonian atmosphere.

The nearshore deposits of the Maywood Formation are overlain by extensive shallow carbonate shelf strata of the Jefferson Formation, likely resulting from a global transgression in the earliest Frasnian. A paired positive and negative $\delta^{13}C_{carbonate\ [carb]}$ isotopic excursion in the Jefferson with a range of >6‰ is a signal of the globally recognized *"punctata"* Event. The unconformably overlying Madison Limestone is lower Carboniferous, except for a thin basal Upper Devonian unit with marine palynomorphs. The Madison regionally records eastward transgression and establishment of widespread marine deposition. It also contains two positive $\delta^{13}C_{carb}$ excursions (up to ∼7.5‰) that make up the mid-Tournaisian (= Kinderhookian–Osagean boundary) carbon isotope excursion (TICE/KOBE). These isotope data provide a framework for regional and global correlation of northern Rocky Mountain strata and an archive of environmental and evolutionary change during the middle–late Paleozoic transition.

INTRODUCTION

Devonian to Carboniferous strata record a critical transition in climate from greenhouse to icehouse condition, the latter including the late Paleozoic Ice Age (Buggisch et al., 2008). This interval was also characterized by dramatic biotic changes in invertebrate fauna (Signor and Brett, 1984; Klug et al., 2010), reef ecosystems (McGhee et al., 2004), tetrapods (George and Blieck, 2011), and both vascular plants (Scheckler, 2001; Meyer-Berthaud et al., 2010) and seed-bearing plants (Falcon-Lang and Bashforth, 2004; Le Hir et al., 2011) with the first emergence of true forests in terrestrial ecosystems (Kenrick and Crane, 1997). This transition in climate was driven, in part, by a steady decline in pCO$_2$, which dropped from more than 1000 ppm in the Early Devonian to perhaps ∼280 ppm in the early to middle Carboniferous (Foster et al., 2017). This decline has been linked to enhanced burial of organic carbon in both coal swamps (Berner and Raiswell, 1983) and marine environments (Caplan and Bustin, 1999). Elevated rates of weathering in uplands due to both active orogenic events and colonization of vascular plants also increased the consumption of atmospheric CO_2, and a concurrent rapid rise in pO$_2$ is recorded in Famennian to Tournaisian strata (Berner and Raiswell, 1983; Algeo and Ingall, 2007).

In this study, we present sedimentologic, paleontologic, stratigraphic, and paleoenvironmental data for Devonian to lower Carboniferous units in northern Wyoming and southern Montana (USA) that allow for reconstruction of the depositional history of the ancient western region of Laurentia. In addition, we provide the first high-resolution $\delta^{13}C_{carb}$ and $\delta^{18}O_{carb}$ chemostratigraphic data for many of these units in this region, which allows for accurate regional and global correlation of middle to upper Paleozoic strata and events.

LOCATIONS AND METHODS

We measured a 5.24-m-thick section through a wide valley-fill deposit of the Maywood Formation at Cottonwood Canyon on the west side of the northern Bighorn Mountains (N44°52′14.0″, W108°03′26.5″), ∼28 km to the east of Lovell, Wyoming (Figs. 1A and 1B). The Maywood rests on both the Middle Ordovician Bighorn Dolomite and a large paleokarst cavity fill of the Beartooth Butte Formation
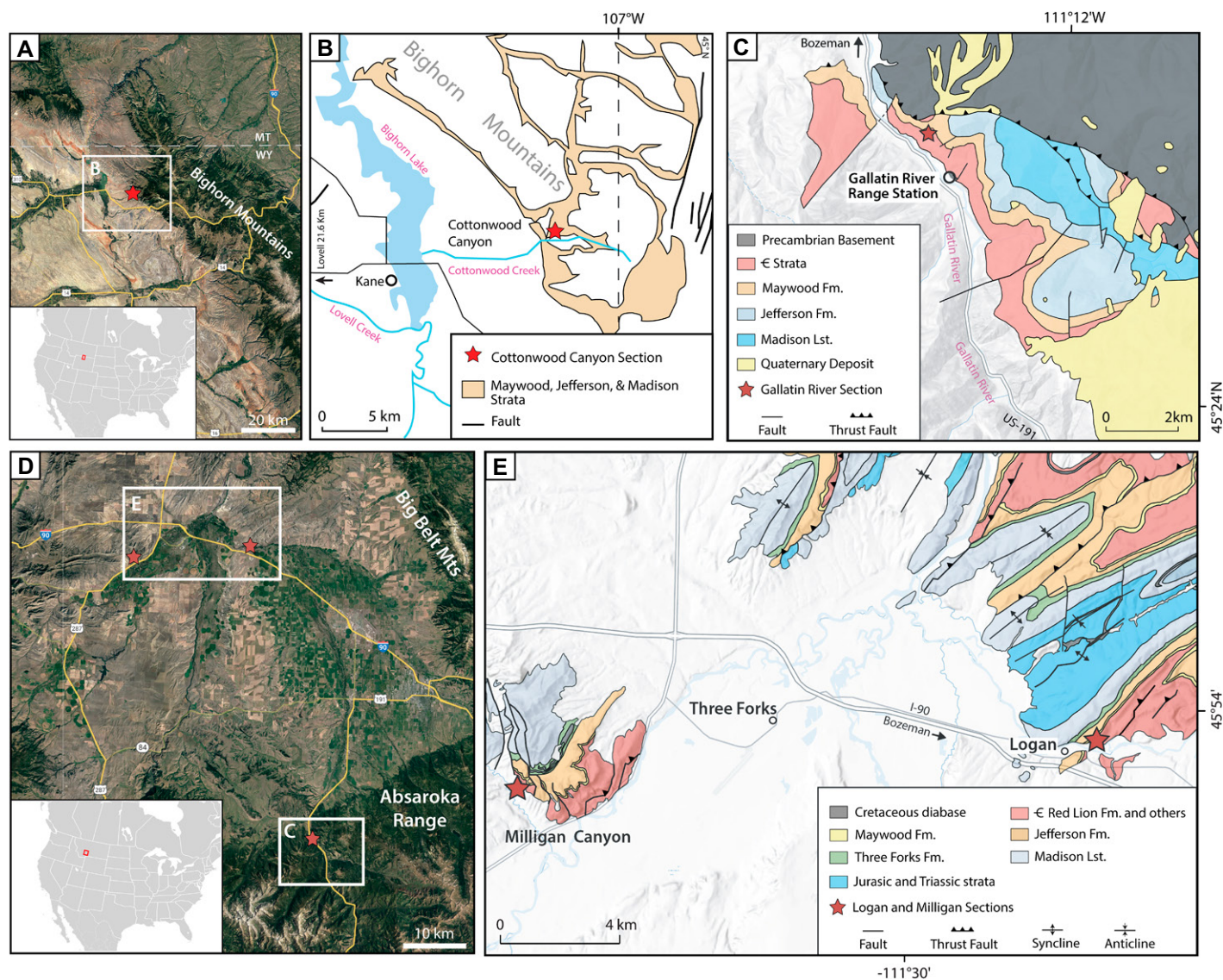
Figure 1. Study area locations. (A) Satellite image of the Cottonwood Canyon section, Wyoming (WY), USA. (B) Generalized geologic map of Cottonwood Canyon area, WY (adapted from Love and Christiansen, 1983). (C) Generalized geologic map of Gallatin River section, Montana (MT) (adapted from Kellogg and Williams, 2000). (D) Satellite image of the Gallatin River section, Logan section, and Milligan Canyon section, MT. (E) Generalized geologic map of the Logan section and Milligan Canyon section, MT (adapted from Vuke et al., 2014). Є—Cambrian; Fm.—Formation; Lst.—Limestone; Mts—Mountains.

(Fig. 2). The overlying Jefferson Formation is 62.3 m thick, and it is in turn overlain by the lower Carboniferous Madison Limestone. We accessed the latter closer to the Cottonwood Canyon trailhead, ~0.5 km into the canyon, on the north wall (N44°52′06.7″, W108°03′38.5″). Two additional sections of the Maywood were measured in Montana (Figs. 1C–1E): (1) in the town of Logan along the Gallatin River (thickness = 15.6 m; N45°53′22.7″, W111°24′56.1″; Figs. 1D and 1E) and (2) in the Gallatin Range near the ranger station 29 km SW of Bozeman (thickness = 10 m; N45°27′44.3″, W111°14′48.7″; Figs. 1C and 1D).

Sections were measured in a bed-by-bed manner with a tape, and covered intervals were measured using a Jacob staff. Detailed sedimentological data were collected from the Maywood and Jefferson formations. Weathering precluded detailed measurement of such data in the Madison Limestone. Carbonate isotope samples were collected every ~0.5 m throughout the Maywood and Jefferson formations from the Cottonwood Canyon, Wyoming, and Logan, Montana, localities. Samples were also taken from the Madison Limestone at Cottonwood Canyon with ~0.5 m sample spacing for the lower 25 m, ~0.75 m spacing for the

25–65 m interval, and ~1 m spacing from 65 m to 181 m.

Carbonate samples were cut with a trim saw and powders were drilled using percussion drill bits on fresh surfaces. Weathering rinds and secondary veins were circumvented. Prepared samples were then analyzed for carbon and oxygen isotopes at Washington University in St. Louis, Missouri, USA. Carbonate powders (~70–110 μg) were reacted with an excess of 100% H_3PO_4 at 72 °C for 4 h within He-flushed, sealed tubes. Released CO_2 was then gathered by a Thermo Scientific Gas Bench II, with the isotopic ratios measured
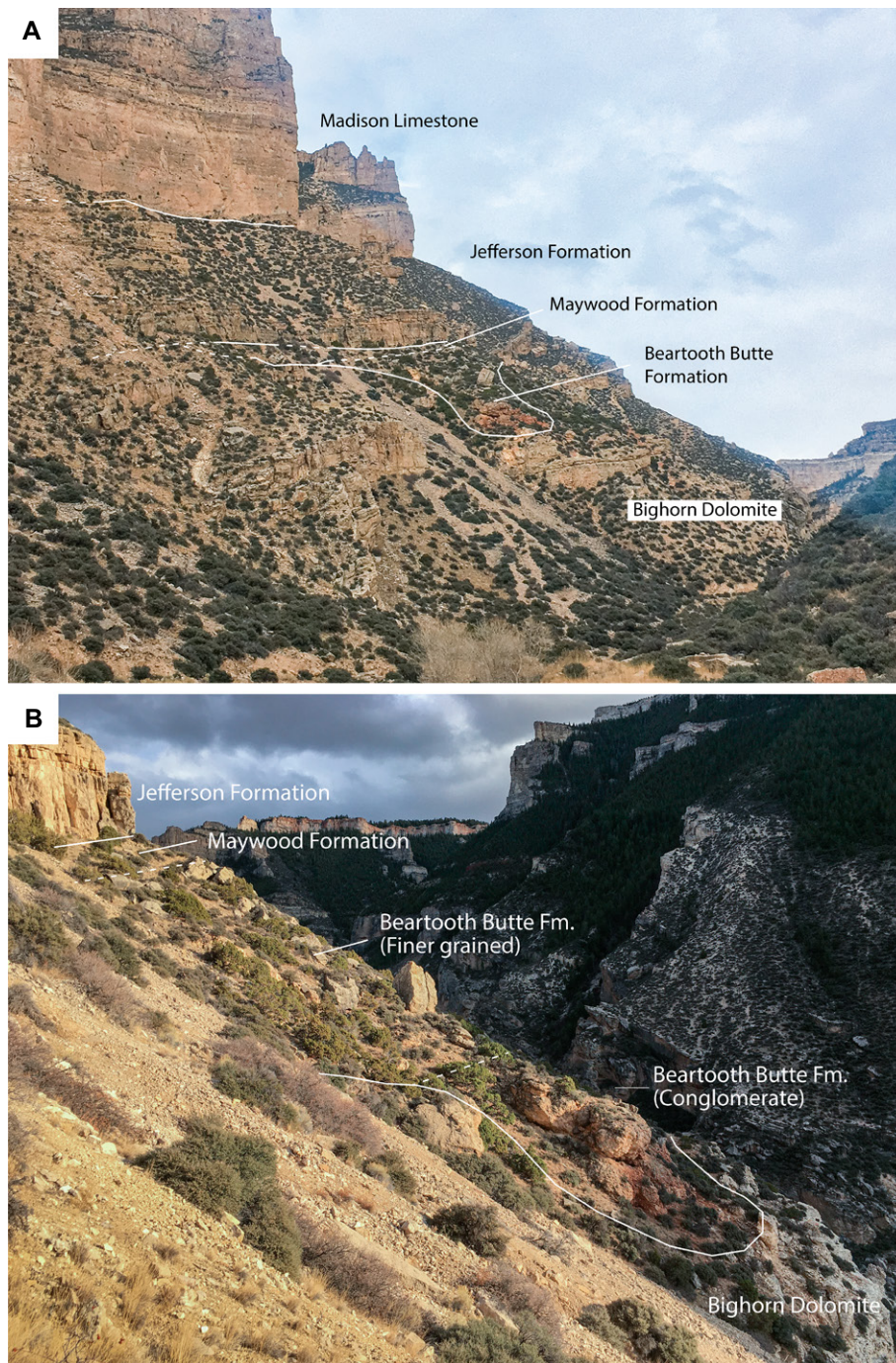
Figure 2. Cottonwood Canyon, Wyoming, USA. (A) North wall of the canyon, looking north-east. Beartooth Butte Formation (Fm.) truncates the Upper Ordovician Bighorn Dolomite. The lower Frasnian Maywood Formation was deposited in a laterally extensive, shallow (5.24 m deep) paleovalley that is cut into the Beartooth Butte Formation near its center and the Bighorn Dolomite at its edges. The Frasnian Jefferson Formation (63.22 m thick) overlies the Maywood Formation, which is overlain by the cliff-forming Madison Limestone (lower Carboniferous). Solid white lines represent observed contacts, and dashed white lines represent inferred contacts. (B) Close-up on the north wall.

for $\delta^{18}O_{carb}$, the precision is $\pm0.219‰$ and the accuracy is $\pm0.273‰$. For isotope data collected at Logan, Montana (Jefferson Formation), the precision is $\pm0.071‰$ and the accuracy is $\pm0.076‰$ for $\delta^{13}C_{carb}$; for $\delta^{18}O_{carb}$, the precision is $\pm0.198‰$ and the accuracy is $\pm0.229‰$. All results, expressed in ‰ notation on the Vienna Peedee belemnite scale, are available in the Supplemental Material[1].

Four samples of organic-rich shale, calcareous shale, and calcisiltite were collected at 3.2 m, 3.5 m, 4.2 m, and 4.53 m from the Maywood Formation, and at 0.46 m of the Madison Limestone from the Cottonwood Canyon locality for palynology. Samples were processed for organic microflora by the Global Geolab in Medicine Hat, Alberta, Canada, prior to analysis. The slides of samples were studied using a Nikon E200 and illustrations taken with a video camera AMU-SCOPE 14 Mp at the Centro de Investigación Científica y de Transferencia de Tecnología a la Producción (CICYTTP), Consejo Nacional de Investigaciones Científicas y Técnicas, Gobierno de la Provincia de Entre Ríos, Universidad Autónoma de Entre Ríos, Argentina, where they are housed under the acronym CICYTTP-Pl. Detailed methods are described in Zatoń et al. (2022) and di Pasquo et al. (2022).

GEOLOGIC BACKGROUND

Paleozoic strata of northern Wyoming were deposited on top of Archaean Wyoming province crust across the ancient Wyoming shelf, which during the early Paleozoic was bounded by the Transcontinental arch to the south and east and the Central Montana trough to the north (Macke, 1993). Devonian through lower Carboniferous strata most commonly rest unconformably above the Upper Ordovician Bighorn Dolomite (Keefer and Van Lieu, 1966) (Fig. 3). Strata of the Beartooth Butte Formation rest within incised valleys across the upper surface of the Bighorn Dolomite (Dorf, 1934; Sandberg, 1961a, 1961b; Sandberg and McMannis, 1964), which were cut at different times in the Early Devonian (Fig. 3) during long-term eustatic lowstands and/or vertical displacements associated with dynamic topography (Gurnis, 1993; Cao et al., 2019) since the region was tectonically quiescent through most of the Devonian (Grader and Dehler, 1999). Previous work by Sandberg and McMannis

by a Thermo Scientific Delta V Plus. The measurements were calibrated under NBS-19, NBS-20, and two in-house standards. Isotopic data from Cottonwood Canyon, Wyoming, yielded a precision of $\pm0.119‰$ and an accuracy of $\pm0.073‰$ for $\delta^{13}C_{carb}$;

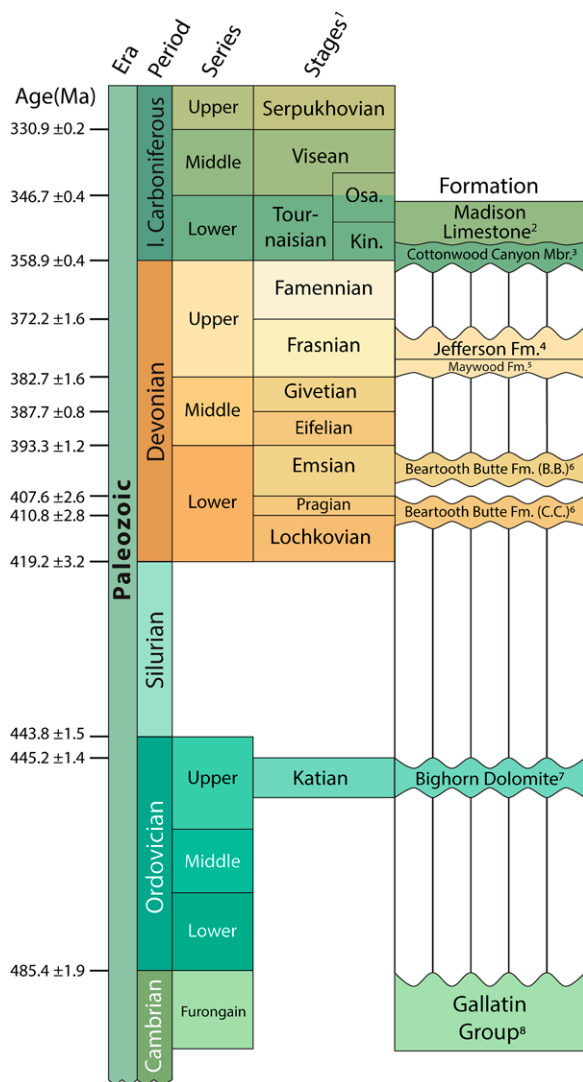**Figure 3. Chronostratigraphic framework and stratigraphic units in the study area in northern Wyoming and southern Montana, USA. Chronostratigraphy after Cohen et al. (2013). Vertical lines represent depositional hiatus between formations. 1—North American stages (Kinderhookian [Kin.] and Osagean [Osa.]) are used for the lowermost (l.) Carboniferous. 2—Peterson (1981). 3—Sandberg and Klapper (1967). 4—Sandberg (1965). 5—Sandberg (1963). 6—B.B. stands for Beartooth Butte, Wyoming; C.C. stands for Cottonwood Canyon, Wyoming; vertebrate fossils by Elliott and Johnson (1997) and Elliott and Ilyes (1996) and spore fossils by Tanner (1984) indicate different ages of two exposures of the Beartooth Butte Formation: Lochkovian–Pragian at Cottonwood Canyon, middle to late Emsian at Beartooth Butte. 7—Holland and Patzkowsky (2009). 8—Deland and Shaw (1956). Mbr.—Member; Fm.—Formation.**

(1964) suggested that the overlying Maywood Formation is a similar valley fill unit. The age of the Maywood was posited by di Pasquo et al. (2022) to be latest Givetian to earliest Frasnian and by Marshall et al. (2022) to be solely Frasnian; our isotopic data (see below) is consistent with the latter (Fig. 3). Shortly after deposition of the Maywood and Jefferson formations the western margin of Laurentia transformed from a passive cratonic margin to an active foreland system of the Antler Orogeny during the latest Devonian to early Mississippian (early Carboniferous) (Silberling and Roberts, 1962; Smith and Ketner, 1968; Johnson and Pendergast, 1981; Speed et al., 1988; Dorobek et al., 1991; Ketner, 2012).

In the Beartooth and Bighorn Mountains of Wyoming, the unconformably overlying Frasnian Jefferson Formation (Fig. 3; Sandberg, 1965) consists solely of the "lower member" (the overlying Birdbear Member is absent). This lower member is equivalent to the Darby Formation in the southern Bighorn Basin and Wind River Range of Wyoming (Sandberg, 1965). The formation is progressively younger and thinner to the east, from Idaho to Wyoming (Grader and Dehler, 1999). The unconformably overlying Madison Limestone of lower Carboniferous age is a thick, cliff-forming carbonate unit that contains a thin latest Devonian Cottonwood Canyon Member at its base (Fig. 3). The Madison generally records eastward transgression and establishment of a marine carbonate system in the Wyoming region during the earliest Carboniferous (North American Kinderhookian Stage; Macke, 1993).
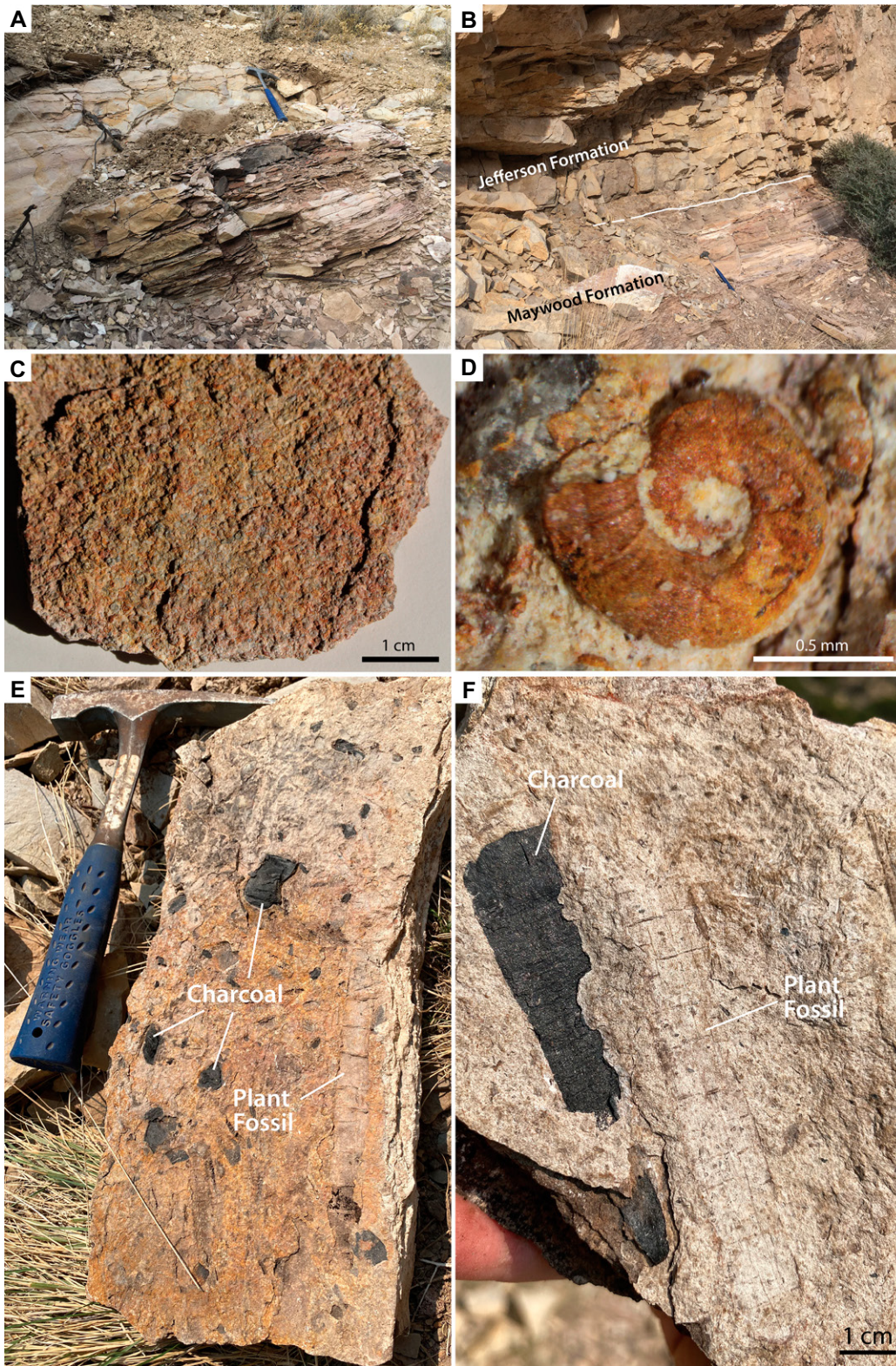
MAYWOOD FORMATION

The Maywood Formation is a yellow-weathering, carbonate-cemented, siltstone-rich unit that outcrops across northern Wyoming and southern Montana. It is highly variable in thickness, ranging from <5 m to >100 m at its type locality in Montana (Sandberg, 1961a). The Maywood unconformably overlies various units regionally and is overlain by the Jefferson Formation, with the contact having been described as conformable (Sandberg and McMannis, 1964). It is broadly correlative with the Souris River Formation of the Williston Basin (Sandberg, 1963) and the lower part of Beaverhill Lake Formation of Alberta Basin, Canada (Kauffman and Earll, 1963). Regional stratigraphic patterns have been interpreted to represent thinning, younging, and onlap of the Maywood from western Montana toward the south and east, with the Cottonwood Canyon section at the southeast limit of exposure of the formation (Benson, 1966).

Cottonwood Canyon

The Maywood Formation at Cottonwood Canyon (Figs. 2–5) is a valley-fill deposit that overlies both the lenticular Lower Devonian Beartooth Butte Formation and the Upper Ordovician Bighorn Dolomite (Sandberg, 1961b; Sandberg and McMannis, 1964). Our studied section of the Maywood Formation rests on the Bighorn and starts with a basal 80 cm unit of yellow-tan weathering siltstone with a few scattered fish fragments. The following 2.2 m of the section is covered. The 1.22 m of strata above the covered interval consists of calcareous shale to shaley calcisiltite and dolosiltite (Figs. 4A and 5). These fine-grained strata are generally dark brown to black, and contain abundant carbonized macerated plant remains and stem impressions, with a few scattered microconchids (~1 mm diameter on average; Fig. 4). A wide variety of floral microfossils exist in these and overlying beds (di Pasquo et al., 2022; Marshall et al., 2022).

The upper 1.02 m of the section consists of calcareous shale, calcisiltite, and <0.5 cm thick gray, tan-weathering, thickly laminated to very thinly bedded, fine to coarse grainstone (Figs. 4B and 5). Beds of microconchid grainstone are present at 4.34–4.5 m, 4.53 m, 4.54 m, and 4.93 m and component allochems consists almost entirely of coiled microconchids (average ~1 mm) (Figs. 4C and 4D); phosphatic fish remains are also present in these grainstone beds. Calcitic and pyrite-coated microconchid tubes, preserved as complete and fragmented specimens, are commonly oxidized and densely packed (Figs. 4C and 4D), and include *Aculeiconchus sandbergi* (Zatoń et al., 2022), a recently described genus and species of microconchids. Large (up to 3 cm), oval-shaped, dispersed coal
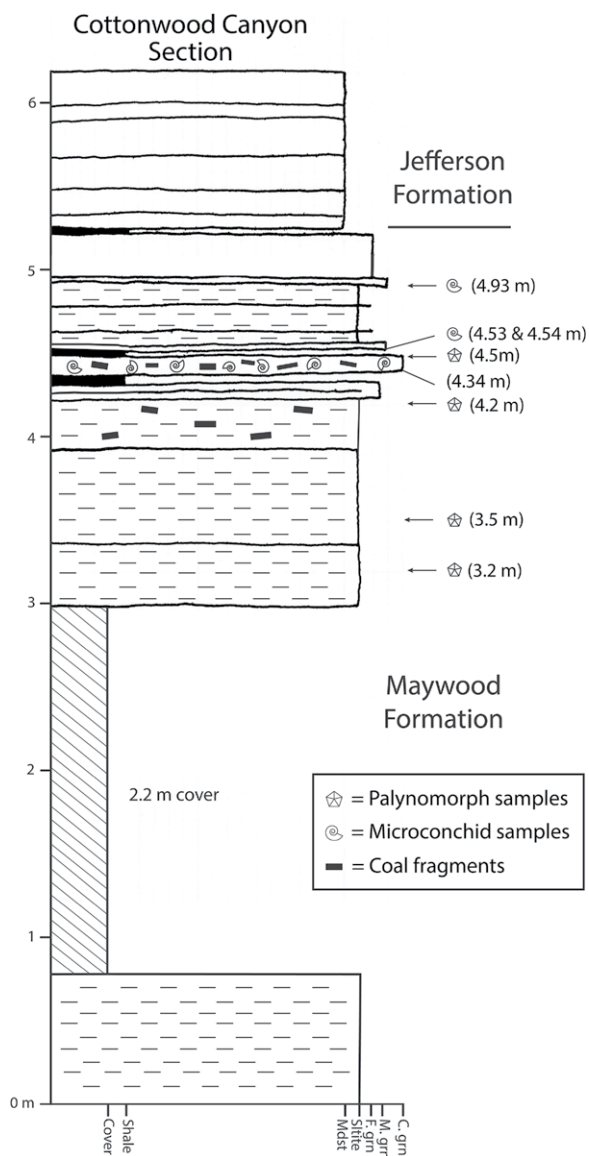
Figure 4. Maywood Formation at Cottonwood Canyon, Wyoming, USA. (A) Strata above the lower 2.2-m-thick covered interval. The lower part of the Maywood is characterized by calcisiltite/ dolosiltite. Abundant carbonized plant debris are present with a few scattered microconchids. (B) Contact interval of the Maywood and the Jefferson formations. Red fine-grained strata of the upper part of the Maywood Formation are overlain by the thin to medium bedded dolomudstone of the Jefferson Formation. (C) Microconchid grainstone from 3.25 m of the Maywood Formation. Microconchids are up to ∼2 mm diameter (average ∼1 mm). (D) An oxidized microconchid from 3.25 m showing transverse riblets on the tube. (E) Bedding plane showing relatively pristine plant stem impressions and charcoal clasts. Hammer for scale. (F) Close-up showing plant stem impression and adjacent charcoal fragment.

pebbles are present, as well as carbonized macerated plant stems and plant impressions. The Maywood Formation is gradationally overlain by dolostone strata of the Jefferson Formation (Figs. 3 and 4B).

Montana Sections

The Maywood Formation at Logan, Montana, is 15.6 m thick and consists of yellow-weathering dolosiltite to very fine dolograinstone with two (15–18 cm thick) shale beds at 3.8 m and 9.2 m (Fig. 6). No marine fossils were noted at this location. The Gallatin Range section of the Maywood Formation SW of Bozeman is ∼10 m thick and locally has more than 5.3 m of relief

Cottonwood Canyon Section

Jefferson Formation

Maywood Formation

2.2 m cover

☆ = Palynomorph samples
◎ = Microconchid samples
▬ = Coal fragments

← ◎ (4.93 m)
← ◎ (4.53 & 4.54 m)
← ☆ (4.5m)
← (4.34 m)
← ☆ (4.2 m)
← ☆ (3.5 m)
← ☆ (3.2 m)

Shale
Cover
Mdst
Sltite
F. grn
M. grn
C. grn

Figure 5. Detailed stratigraphic column of Maywood Formation at Cottonwood Canyon, Wyoming, USA. The vertical axis is stratigraphic height (in meters). The Maywood Formation overlies the Bighorn Dolomite and is overlain by the Jefferson Formation with a sharply gradational or slightly disconformable contact. Numbers on the right indicate stratigraphic heights where microconchid and microspore samples were taken. Mdst—mudstone; Sltite—dolosiltite; F. grn—fine grainstone; M. grn—medium grainstone; C. grn—coarse grainstone.

along its basal unconformity surface, which rests on the Cambrian Red Lion Shale (Sandberg and McMannis, 1964; Fig. 6). The lower 1.7 m of our section of the Maywood at this location consists of green to gray, fissile shale interbedded with minor, parallel laminated, 4- to 6-cm-thick dolosiltite beds, and a few <5 cm thick, calcisiltite-filled gutter casts (Fig. 6). The next 3.3 m (from 1.7 m to 5 m) is a complex interval dominated by massive, light gray, yellow weathering, fine grainstone. The grainstone locally contains a few intervals with scattered black chert clasts, and two beds (50 cm and 35 cm thick at 2.86 m and 4.7 m, respectively) with abundant silicified clasts up to 6.5 cm across. There are also two beds (5 cm and 15 cm thick) of shaley siltstone with dispersed very coarse sand- to granule-sized quartz grains (at 2.4 m and 5.0 m). The upper 5 m of the section consists of finely laminated

dolosiltite and very fine-grained, massive grainstone. Only a few beds in this interval contain scattered quartz grains. There is a <3-cm-thick horizon of possible solution breccia at 6.5 m, and <0.5-cm-deep shrinkage cracks at 6.78 m.
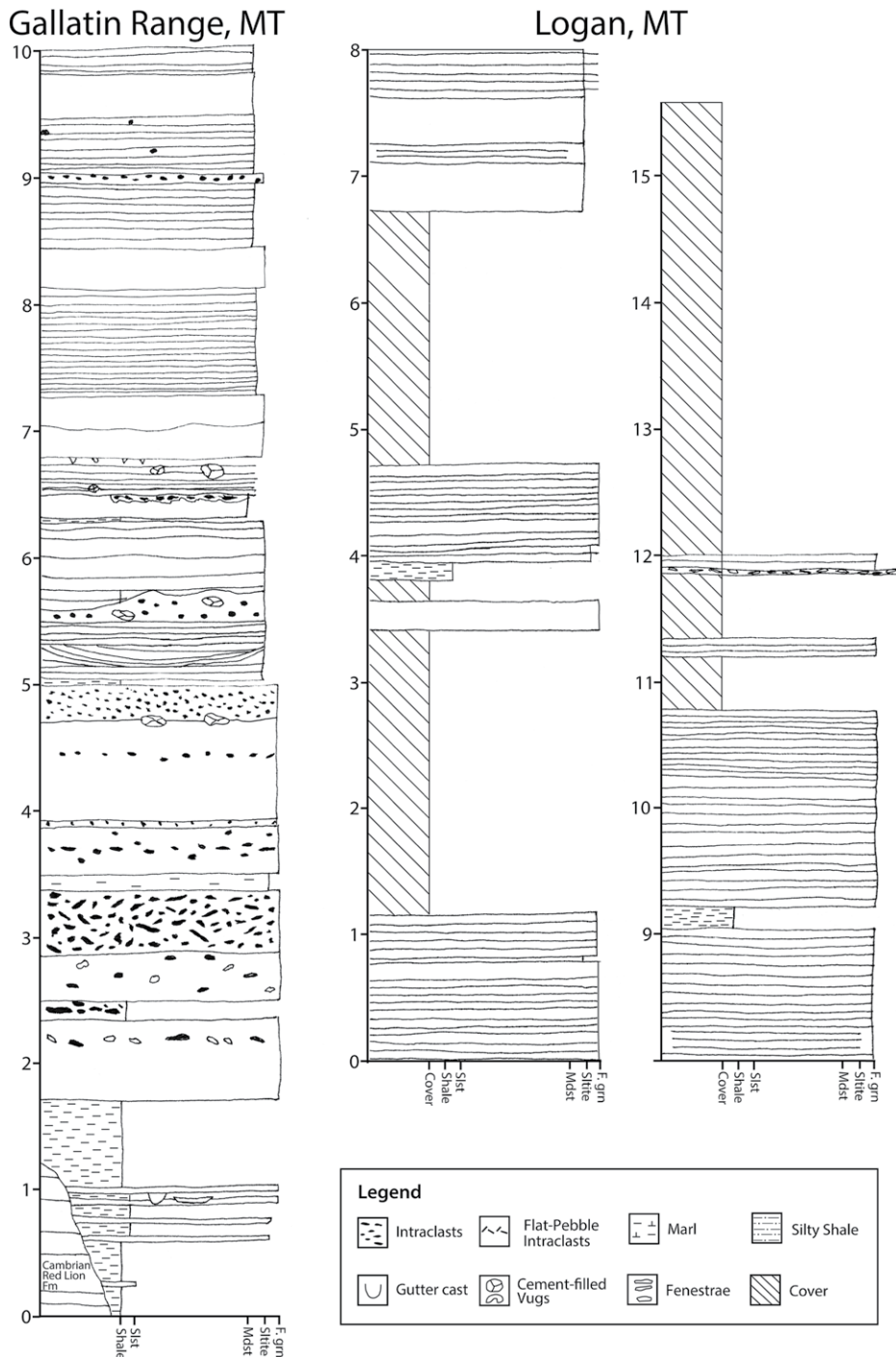
Vertebrate Paleontology

Photomicrographs taken by one of us (MZ) of phosphatic fish fossils in several samples collected from the microconchid grainstone beds reveal the presence of a variety of crown- and stem-group gnathostomes. Chondrichthyans are evident from tooth crowns (Fig. 7A) with characteristic keels or cristae extending from apex toward the tooth base. One example (Fig. 7A) aligns with the broad class of shark teeth described as "cladodont," but also matches quite closely examples known from members of the

Symmoriiformes. One scale (Fig. 7B) is chondrichthyan and another possibly acanthodian—the distinction between these designations is increasingly arbitrary, sometimes little more than size-based, as the latter are now recognized as stem grade and included within the former. The persistent presence of stem-group jawed vertebrates is suggested by fragments, including one specimen (Fig. 7C) with a "sawtooth" edge as a series of slightly irregularly spaced dermal denticles that shows some degree of base overlap. This imprecise pattern is known from the crests, rims, and keels of dermal skeletal plates in antiarch placoderms, such as the extremely widespread antiarch genus *Bothriolepis*. Densely packed fields of tiny denticles are difficult to attribute with confidence, and one example (Fig. 7D) very likely represents part of a larger structure. Lastly, ray-finned fishes, Actinopterygii, are represented by likely teeth and fulcral scales (Figs. 7E and 7F, respectively). Teeth are attributed based on the distinctive cap on the crown apex. In one example (Fig. 7E), the shoulder surrounds the crown, where the tooth surface angles quite sharply toward the apex, and the tooth appears near circular in cross section from base to apex, unlike the cladodont tooth, which exhibits slight labio-lingual flattening. Lastly, the scales and scale fragments include at least one example of an actinopterygian fulcral scale (Fig. 7F), likely from close to the base of the leading edge (cutwater) of a fin. The example shown is symmetrical around its long axis, with simple ornament on the exposed surface and a slight depression in the midline where it would be overlapped by the adjacent member of the fulcral series. An assemblage of fish plates and fish teeth was noted by Sandberg (1963) for the Maywood Formation at this same locality, although no photographs were presented. Marshall et al. (2022) also described some fish remains from this locality, including sarcopterygian pieces and a possible tetrapodomorph fish scale.

Plants and Charcoal

The Maywood Formation contains several horizons of sandstone, siltstone, and grainstone with abundant plant fossils. The plant remains are mostly comprised of stems (Figs. 4E and 4F) that locally display discontinuously preserved vasculature and sporadically preserved large 5-cm-wide (megaphyllous?) leaves, both of which are preserved as allochthonous and disarticulated compressions. Common and conspicuous charcoal clasts with 3-D preservation exist along with the plant compression fossils in these beds (Figs. 4E and 4F). In contrast with the plant compressions, the charcoal clasts are extremely soft, are low density, and have a dark black

Figure 6. Detailed stratigraphic section from the Gallatin Range locality near the ranger station, 29 km southwest of Bozeman, Montana (MT), USA, and one from the town of Logan along the Gallatin River near Three Forks, MT. The vertical axis is stratigraphic height (in meters). Slst.—siltstone; Mdst—mudstone; Sltite—dolosiltite; F. grn—fine grainstone.
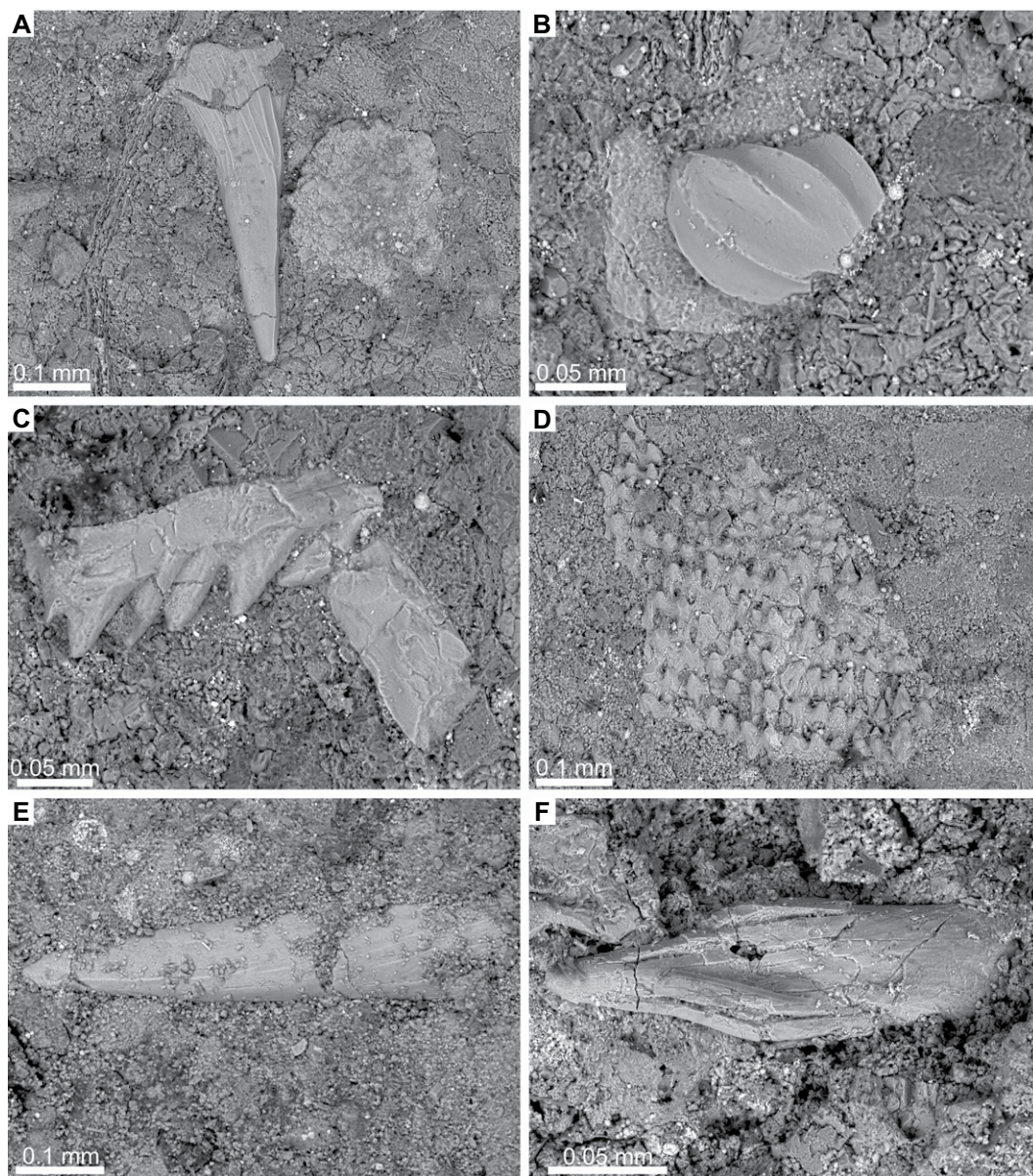
Microfossils

Zatoń et al. (2022), in a preliminary palynologic analysis of Maywood microfossils, identified terrestrial spores of lycopsids, primitive fern groups, and progymnosperms. Di Pasquo et al. (2022) and Marshall et al. (2022) provided a more detailed analysis of the palynotaxa. Based on the presence of microspore species *Samarisporites triangulatus* and *Contagisporites optivus*, di Pasquo et al. (2022) assigned the Maywood Formation fossil assemblage to the *C. optivus*/*S. triangulatus* palynozone, a relatively long zone that spans the late Givetian to early Frasnian. Climatic changes associated with the late Givetian Taghanic event caused significant faunal/floral extinctions (Algeo and Scheckler, 1998; Turnau and Racki, 1999; Aboussalam, 2003; Aboussalam and Becker, 2011; Marshall et al., 2011; Turnau, 2011, 2014), including reductions in archaeopterids and aneurophytes (di Pasquo et al., 2022). Such extinctions did not affect flora lived far from shore, which were better adapted and had higher survival rates (Marshall et al., 2011; Turnau, 2014; Stein et al., 2020). The landward setting for the Maywood at Cottonwood, and the high abundance and low diversity of archaeopterids progymnosperm (e.g., *G. lemurata* and *C. optivus*), led di Pasquo et al. (2022) to thus prefer a late Givetian age for the unit. This age preference was also supported by the absence of lower Frasnian spore species such as *Chelinospora concinna*, *Verrucosisporites bulliferus*, *Cirratriradites jekhowskyi*, and *Lophozonotriletes media*, which were used to establish the Givetian–Frasnian boundary in the Ardenne region of Europe (Streel et al., 2021). The Upper Devonian prasinophyte *Maranhites* (González, 2009), which globally co-occurs with land-derived palynomorphs in shallow, near-shore marine deposits, is also absent.

Marshall et al. (2022) provided an alternative explanation, namely that the Maywood fauna is potentially Frasnian, an interval with generally greater floral diversity. In their view, the depauperate fauna of the Maywood Formation would have been linked to environmental factors, namely, a stressed very shallow water setting (see Zatoń et al., 2022; di Pasquo et al., 2022). Although biostratigraphic data cannot resolve the age at present, our chemostratigraphic analysis (see below) supports a lowermost Frasnian age for the formation. This would suggest that deposition of the Maywood at Cottonwood Canyon would have taken place during the IIb transgression (Johnson and Sandberg, 1988).

Depositional Environment

Based on the presence of *Bothriolepis* fish fossils, Sandberg and McMannis (1964)

streak. These also exhibit brittle deformation, are subrounded to rounded, have low to high sphericity, and are sub-mm to 10 cm long, all of which are features consistent with limited downstream transport in a fluvial system. We found no in situ plant fossils in the Cottonwood Canyon

exposure of the Maywood (see di Pasquo et al., 2022). The taxonomic identities of the plants are uncertain, though some of the large stems and leaves may have progymnosperm, lycopsid, and early fern affinities (Beck, 1966; Stewart and Rothwell, 1993; Gensel and Edwards, 2001).

Figure 7. Phosphatic fish fossils from the microconchid grainstone of the Maywood Formation at Cottonwood Canyon, Wyoming, USA. (A) Chondrichthyan tooth crown, likely derived from symmoriid. (B) Skin denticle/scale of acanthodians. (C) Closely packed denticles from the trailing edge of a fin spine or a dermal skeletal plate from a keel of an antiarch placoderm. (D) Field of denticles of larger structure. (E) Tooth of Actinopterygian (ray-finned fish). (F) Fulcral scale of Actinopterygian.

suggested that the Maywood Formation at Cottonwood Canyon was likely deposited in a marginal marine, brackish to freshwater environment, like the valley-fill deposit of Beartooth Butte Formation. The large aggregation of monospecific microconchids, and simultaneous absence of other benthic fossils, suggests a possible stressed paleoenvironment, but like fish fauna, they are unable to be used as unequivocal paleosalinity indicators (Zatoń et al., 2012). The palynoflora assemblage is dominated by spores and megaspores, including progymnosperms, which were major components of swamp plant communities. Along with spores of terrestrial herbaceous and shrubby lycopsids, and primitive ferns, the overall floral assemblage indicate that the Maywood channel was in very close proximity to freshwater settings (fluvio-lacustrine, lower floodplain, or paralic). The assemblages also yielded (1) a few brackish/marine prasinophyte algae, *Quadrisporites* and *Dictyotidium*; (2) tetrads; (3) minor pyrite; and (4) fine granular and fibrous amorphous organic matter with orange fluorescence (di Pasquo et al., 2022), all of which support a brackish, shallow water setting (Zatoń et al., 2022; di Pasquo et al., 2022), as suggested by Sandberg (1963). The preservation of the microconchids as pyritic steinkerns in places, suggests anaerobic early diagenetic conditions and a source of sulfate, the latter of which is consistent with brackish water conditions.

We agree with Marshall et al. (2022) that the Maywood setting was a "…low-energy, fully subaqueous…" setting. However, their interpretation of the very thin to thin grainstone beds as upper shoreface deposits of a wave-dominated coast is unlikely, even if the shoreface was low energy, as they suggest. The Maywood is dominated by calcisiltite and the very thin grainstone beds are intercalated with thin shale beds. Shoreface deposits consist of meters to tens-of-meters of generally medium to thick bedded, cross-stratified, parallel laminated, and hummocky cross-stratified sandstone that lack shale interbeds (Olsen et al., 1999; Wesolowski et al., 2018; Li et al., 2021). The abundance of siltstone, ripple scale of lamination, and shale interbeds are inconsistent with facies models for wave dominated upper shorefaces. The grainstone beds of the Maywood Formation are <1 m below the

marine Jefferson Formation, which extends in all directions across and well beyond the Maywood incised valley. Thus, during deposition of the upper Maywood, the valley would have had ~1 m of residual relief within a valley that was <~100 m wide. Based on reconstructions of the paleoshorelines at this time, the Maywood Formation valley at the Cottonwood Canyon location would have been >100 km away from the open ocean (Grader and Dehler, 1999; Hofmann, 2020; Marshall et al., 2022). Waves would not likely have propagated far into the upper reaches of a >100-km-long, shallow incised valley, and given the depth and width, wave attenuation due to friction would have been substantial (Madsen et al., 1988). Small waves due to local winds might have reworked the microconchids into grainstone beds, but the limited fetch of the incised valley and shallow depths would have severely limited wave heights and energy levels.

It is unclear if the position of the Maywood valley was in any way influenced by inherited topography associated with the older Beartooth Butte valley, which is located ~1 km to the east-southeast of our Maywood section in Cottonwood Canyon (Elliott and Johnson, 1997; Caruso and Tomescu, 2012), and was filled during the Lochkovian–Pragian (Sandberg, 1961b; Tanner, 1984; Caruso and Tomescu, 2012), ~30 m.y. before the lower Frasnian Maywood Formation was deposited. One possibility is that the fine-grained deposits of the Beartooth Butte Formation filled the valley topography at that time, but during the subsequent ~30 m.y. new rivers were initiated in a similar location, in part due to preferential erosion of the silty Beartooth Butte valley fill relative to the older Bighorn Dolomite into which the Beartooth Butte Formation was incised. More locally, the Maywood valley fill rests directly above a narrow, deep Beartooth Butte Formation paleokarst cavity fill, and either residual topography or the easily eroded uppermost fill of that cavity may have influenced its position. In any case, the reappearance of nearly identical lithofacies and fossil assemblages of microconchids, plant debris, cartilaginous and fragmented bony fossils, and microspores (Elliott and Johnson, 1997; Caruso and Tomescu, 2012; Zatoń et al., 2022; di Pasquo et al., 2022) suggests that low-diversity, estuarine fauna likely filled salinity-stressed niches and tracked marine incursions into valleys that were cut during previous lowstand conditions, and that this pattern was repeated during the Early to Late Devonian. The general tectonic quiescence of this interval, and the fact that bedrock incised valleys are typically associated with areas of tectonic uplift (Burbank et al., 1996), suggest that eustasy and/or uplift associated with dynamic topography (mantle flow; Flament

et al., 2013) was a driver of these repeated events of valley incision and deposition.

The presence of plant fossils and plant-derived charcoal in the Maywood Formation provide a sedimentary record of an early Late Devonian terrestrial landscape adjacent to the Maywood valleys, which was rich in woody shrubs and co-evolving with fire events. Fire is a critical Earth surface process (Bowman et al., 2009), and sedimentary charcoal provides both a fossil metric of the burning of ancient biomass (Glasspool et al., 2015) and a constraint on the dioxygen content of Earth's atmosphere at the time of deposition (Scott and Glasspool, 2006; Glasspool and Scott, 2010; Fischer, 2016; Fischer and Valentine, 2019). Charcoal is a pyrolytic product of wildfire and thus it provides a measure of combustion (Chaloner, 1989; Scott et al., 2013). The oldest known charcoal is upper Silurian (Glasspool et al., 2004), and it forms a record that parallels the evolution of plants and establishment of terrestrial ecosystems throughout the Devonian (Harland et al., 1976; Lapo and Drozdova, 1989; Goodarzi and Goodbody, 1990; Volkova, 1994; Cressler, 2001; Kennedy et al., 2013).

There are longstanding questions about the history of O_2 throughout the Paleozoic and its relationships to animal and plant evolution (Algeo and Scheckler, 1998; Berner, 2006; Algeo and Ingall, 2007; Dahl et al., 2010; Lenton et al., 2016; Wallace et al., 2017). The widespread presence of charcoal in the Maywood Formation provides useful bounds on ancient atmospheric O_2 during the earliest Late Devonian. The late Emsian to Givetian is considered to record a "charcoal gap," although there is almost no record of charcoal in the Frasnian except microscopic charcoal fragments in a single lower Frasnian coal, despite rapid diversification of the woody tree *Archaeopteris* in the Frasnian (Scott and Glasspool, 2006; Glasspool et al., 2015; Lu et al., 2021). Experiments and calculations have revealed that below an atmospheric O_2 content of 16% by volume (assuming a mass of 1 atmosphere) fire will not spread regardless of the moisture content of the vegetation, which establishes a lower limit to the fire window (Cope and Chaloner, 1980; Chaloner, 1989; Belcher et al., 2010, 2013; Watson and Lovelock, 2013). Our results indicate that earliest Late Devonian O_2 exceeded this lower threshold, and that fire and charcoal production took place during the interval hypothesized to have no macroscopic charcoal. This O_2 constraint underscores the importance of the tight, and poorly understood, biogeochemical feedbacks that maintained atmospheric O_2 levels over much of Phanerozoic Earth history, even despite its extremely short (~700-year) residence time (Fischer and Valentine, 2019).

JEFFERSON FORMATION

The Jefferson Formation is well exposed in areas of Idaho, Montana, and Wyoming (Fig. 8A), with spatial variations of lithologies (Sandberg, 1965; Grader and Dehler, 1999; Grader et al., 2017). Sandberg and Poole (1977) noted a higher content of siliciclastic detritus in the formation in south-central Montana, and they ascribed the increased siliciclastic sediment influx to the E-W–trending Central Montana Uplift and the Yellowstone Uplift, which are two paleo-highs formed during the early stages of the Antler Orogeny.

The formation is progressively younger and thinner to the east, from Idaho to Wyoming (Sandberg et al., 1988; Grader and Dehler, 1999; Grader et al., 2017). The total thickness of the lower member of the Jefferson Formation, specifically, decreases southeastward, from Montana (~200 m) to the Bighorn Mountains, Wyoming (~70 m), where it reaches the southernmost extent of deposition (Sandberg, 1965). Johnson et al. (1985) assigned parts of the Jefferson Formation in central Idaho to conodont zones ranging from *Polygnathus varcus* to *Palmatolepis triangularis*, which span the mid-Givetian to lowermost Famennian stages. Sandberg (1965) and Sandberg et al. (1988) assigned a Frasnian age to the lower member of the Jefferson in most parts of Montana and Wyoming. The Jefferson Formation at Cottonwood Canyon section was assigned to the *hassi* Zone by these authors based on lithological correlations to sections in Montana. Little or no conodont data have been published on Jefferson exposures in the Bighorn Mountains. We provide a detailed measured section from Cottonwood Canyon, Wyoming, where the strata are well preserved and diagenetic alteration is minimal (Fig. 9). Chemostratigraphic data from this section and from a section at Logan, Montana, are presented below, although for the latter no detailed stratigraphic section is presented because the strata are heavily weathered and little primary sedimentary structures are preserved.

Description

The Jefferson Formation consists primarily of gray to tan weathering, very thin to thick bedded dolograinstone, dolomudstone, dolosiltite, and marl. These lithologies locally (e.g., fine grainstone at 46.16 m) contain 5%–10% dispersed frosted silt to medium sand quartz grains, as well as minor feldspar and glauconite (Fig. 8D), although in a few beds of dolosiltite (e.g., 47.48 m, 55.17 m) quartz make up ~50% of the rock.
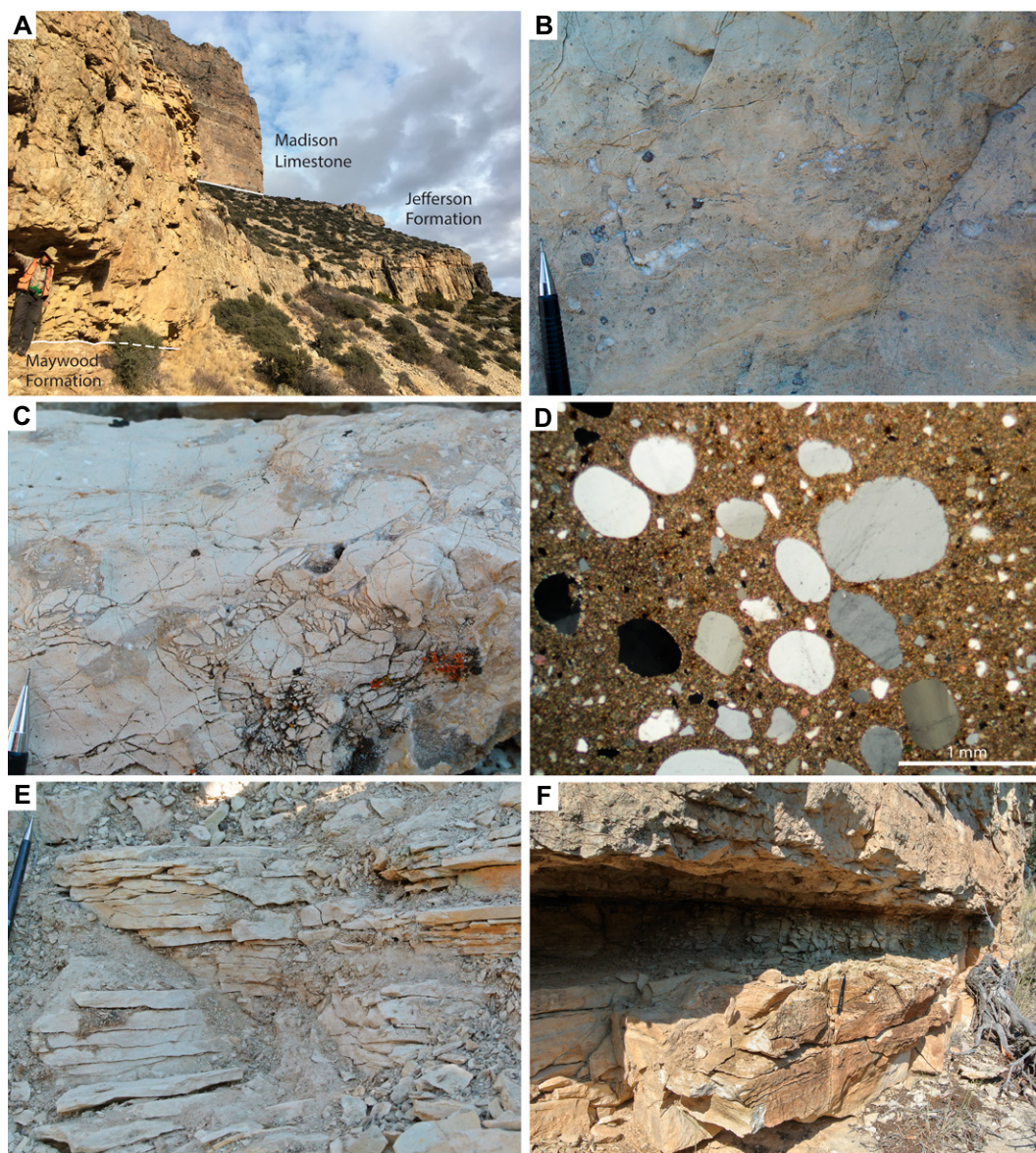
Figure 8. Jefferson Formation at Cottonwood Canyon, Wyoming, USA. (A) The Jefferson Formation and overlying cliff-forming Madison Limestone. (B) Irregular fenestrae filled with calcite cement at 9.1 m. (C) Small-scale paleokarst filled with breccia and calcite cement at 9.1 m. (D) Sandy dolomudstone at 48.82 m of the Jefferson Formation under cross-polarized light. Rounded to well-rounded, frosted quartz grains are present in a micritic matrix. Minor amount (<5%) of feldspar and glauconite are also present. (E) Flaggy-weathered dolosiltstone beds at 14.12 m. (F) A 38-cm-thick, quartz-cemented sandstone at 8.72 m. Pencil is 14 cm long and pencil tip is 2 cm long, for scale.

The dolomudstone beds are primarily 1–2 cm thick and commonly contain fenestrae (e.g., at 9.1 m to 9.9 m, and at 28.62 m and 47.98 m; Figs. 8B and 9) and calcite-cement filled vugs, particularly in the ∼1.0–9.0 m interval, although they are present throughout (Fig. 9). The fenestrae are filled with calcite and have both flat (laminoid) and irregular geometries. Flat types are characterized by flattened, curved to planar, subparallel pores that are typically 1–5 mm thick and less than 20 mm long. The irregular fenestrae are scattered, nearly equidimensional pores (birdseyes) that typically ranges from 1 mm to 5 mm in diameter (Fig. 8B). The dolosiltite is very thin to thinly bedded (average 1–5 cm) and tends to be flaggy-weathering and poorly exposed (Fig. 8E). One bed, at 8.72 m, consists entirely of thin to medium bedded, medium- to coarse-grained quartz sandstone (Figs. 8F and 9), which is sharply overlain by fenestral dolomudstone. There is also a single bed (at 28 m) of purple to dark red, near-clast-supported, flat pebble (average ∼1 cm) conglomerate with subrounded to subangular dolosiltite clasts.

Paleokarst cavity fills are also present in the Jefferson dolomudstone beds and are filled with calcite cement, breccia, and red dolosiltite (Fig. 8C). These include tubular to lenticular dissolution vugs (average 1–7 mm), some of which are filled with calcite cement, siliciclastic silt, and endogenetic breccia. The breccia is clast-supported, with clasts that are subangular to subrounded, and show mosaic and crackle fabrics suggestive of in situ derivation and disintegration. Sizes of the breccia clasts range from granule to pebble (Fig. 8C), and there is locally a bimodal distribution of clast sizes. Many cavity-fills of breccia at 9.1–10.0 m are vertical pipes with collapse breccia.

Stratigraphic Patterns

The lower 8.72 m of the Jefferson Formation, above its gradational contact with the Maywood Formation, is highly vuggy dolomudstone facies, and the upper 2 m of this interval is intensely karsted with cavities filled with breccia, dolosiltite, and calcite cement (Fig. 9). This is directly overlain by the 38-cm-thick quartz sandstone unit.

This is followed by a massive bed of vuggy dolomudstone facies with fenestrae at 9.1 m. An upward-coarsening succession exists from 9.9 m to 28 m, where the facies changes from
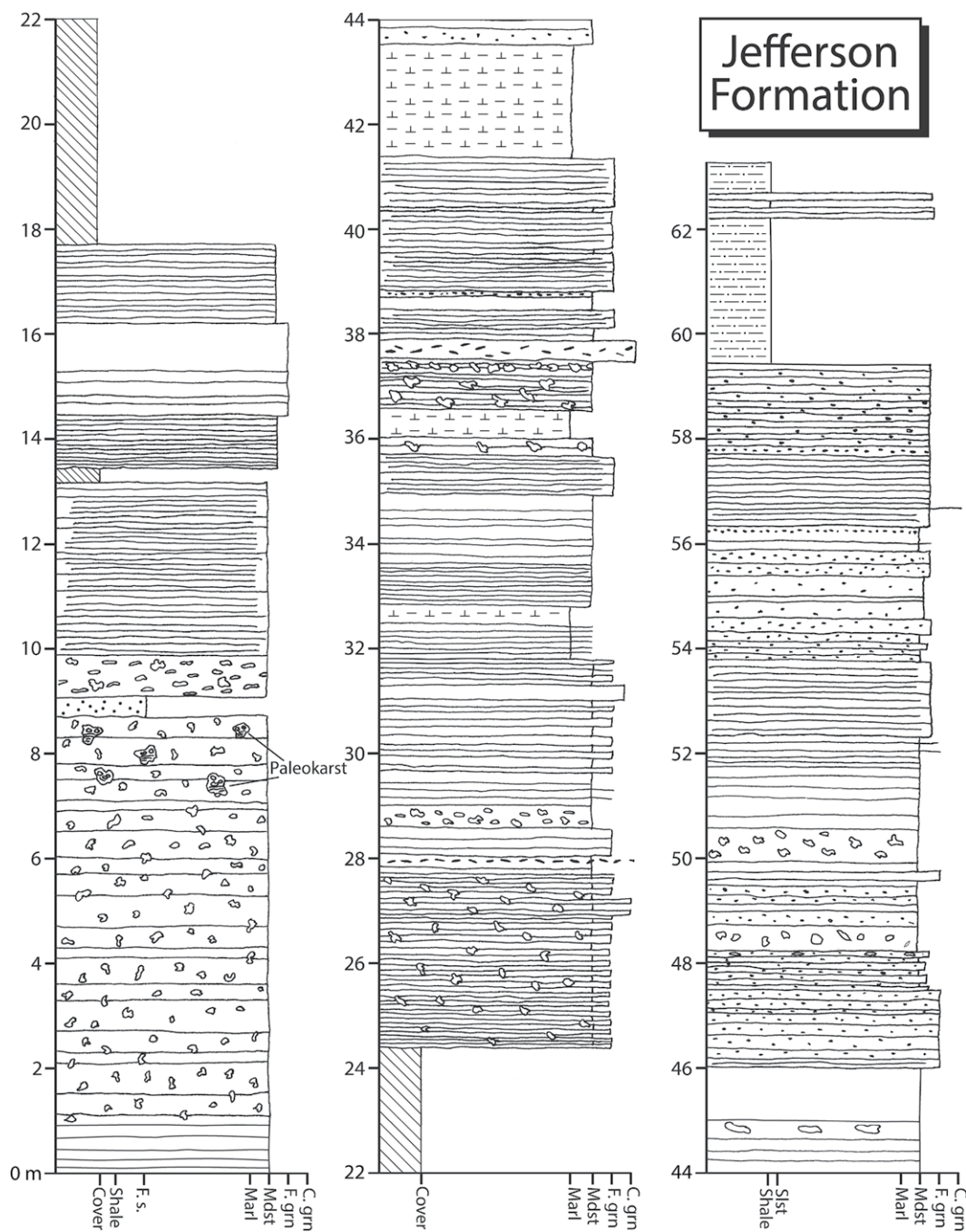
Figure 9. Detailed stratigraphic column of Jefferson Formation at Cottonwood Canyon, Wyoming, USA. The vertical axis represents stratigraphic height (in meters). Legend provided in Figure 6. F. s.—fine sandstone; Mdst—mudstone; F. grn—fine grainstone; C. grn—coarse grainstone; Slst.—siltstone.

massive dolomudstone, to flaggy dolosiltstone, then to coarse dolograinstone and vuggy dolomudstone (Fig. 9). This is capped by the flat pebble conglomerate bed at 28 m. Several similar 2- to 4-m-thick coarsening-upward cycles are present above 28 m. These show facies changes from non-vuggy dolomudstone and dolosiltstone to fine to coarse dolograinstone, and they are overlain by silty marl or dolomudstone (Fig. 9). The dolomudstone at the caps of these cycles contain abundant vugs or fenestrae. These are sharply overlain by non-vuggy, fenestrae-free dolomudstone, dolosiltite, or marl.

Cycle tops above 47.98 m commonly have dispersed medium to coarse, frosted quartz grains. The section from 50.49 m to 63.23 m shows a facies change from dolomudstone to sandy dolosiltite and then silty shale, with an upward-increasing percentage of quartz grains (Fig. 9). Many beds contain dispersed frosted quartz (average 30%) in the upper part of this interval, and one bed of coarse quartz sandstone with frosted grains is present at 56.44 m.

Depositional Environments

The Jefferson Formation at Cottonwood Canyon has a notable absence of depositional sedimentary features such as wave ripples, cross-bedding, sole marks, or mud cracks. Fossils are not abundant, and there are only limited biogenic sedimentary structures (e.g., cryptomicrobial laminite). The dolomitized facies all represent a generally shallow, inner carbonate shelf that shows no evidence of significant wave- or tidal-diagnostic sedimentation. Relative water

depths were reconstructed, based primarily on the distribution of sandstone beds and both shallow water and subaerial exposure features (i.e., fenestrae and paleokarst) (Fig. 10).

In general, the dolograinstone was likely deposited in shallower environments than the glauconite-bearing shelf dolomudstone facies. Interbeds of dolograinstone with dolomud-

stone may represent event beds, although the general lack of visible stratification makes it difficult to discern the nature of the (presumed) higher energy flows. The marl facies may have formed in comparatively distal quiescent areas where carbonate production tailed off. These more distal regions of the shelf received terrigenous clay from point sources along the

length of the carbonate platform and/or from eolian sources.

The coarsening upward cycles of the Jefferson are interpreted as shoaling successions from deeper marl facies through to intensely karsted carbonate (Fig. 10). Basal deposits of shoaling cycles contain massive, non-vuggy facies such as dolomudstone, marl, or dolosiltite. Cycle
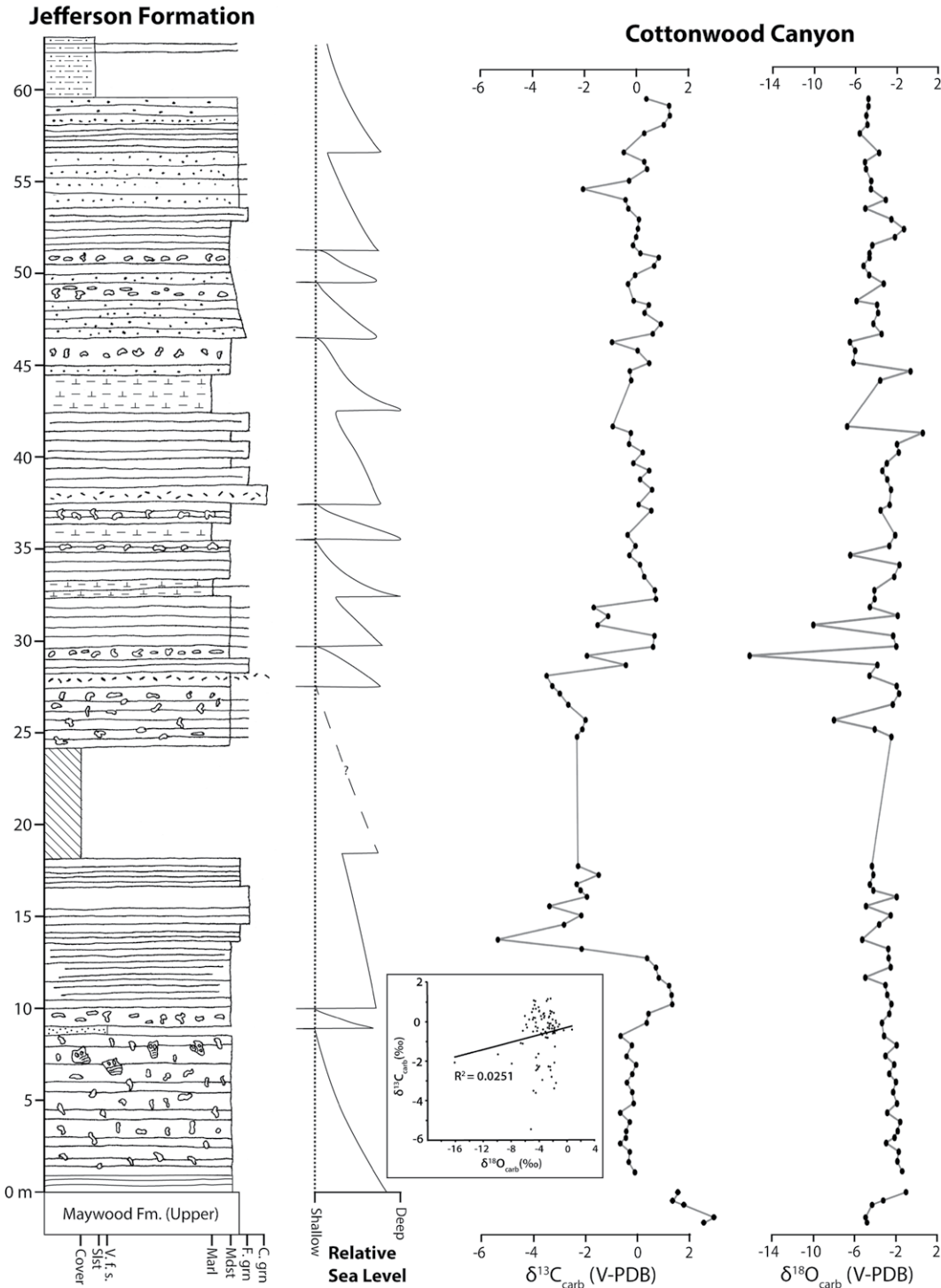
Figure 10. Generalized stratigraphic column, interpreted sea level curve, and δ¹³C_carbonate [carb] and δ¹⁸O_carb stable isotope data (‰ Vienna Peedee belemnite [V-PDB]; n = 96) for the Jefferson Formation (Fm.) at Cottonwood Canyon, Wyoming, USA. The vertical axis represents stratigraphic height (in meters). The total measured thickness of the section is 63.22 m. The inset shows the cross plot of δ¹³C_carb and δ¹⁸O_carb data. Solid line is best-fit linear regression with coefficient of determination (R²) = 0.0251. Legend provided in Figure 6. Slst.—siltstone; V. f. s.—very fine sandstone; Mdst—mudstone; F. grn—fine grainstone; C. grn—coarse grainstone.

caps contain paleokarst, fenestrae, and abundant quartz sand. The fenestrae are typical features of peritidal environments (Shinn, 1983; Tucker and Wright, 1990), which form from entrapped gas bubbles released by the growth and decay of microbes (Tucker and Wright, 1990) in near surface deposits of shallow water settings (i.e., low lithostatic and hydrostatic pressures). The frosted and well-rounded quartz grains may indicate transport of eolian quartz grains from nearby dunes. Cycle boundaries record transitions from subaerial exposure to basal transgressive deposits formed during initial flooding of the subaerially exposed surfaces. The paleokarst records subaerial diagenetic dissolution and precipitation of carbonate and marks the position of unconformities (Canter et al., 1992; Cooper and Keller, 2001; Kervin and Woods, 2012). The clast-supported nature and the abundance of mosaic to crackle breccia support a cave-ceiling collapse mechanism of breccia formation, which is indicative of vadose-zone dissolution of the pre-karsted carbonate strata (Loucks, 1999). The moderate to high degree of rounding for karst breccia at ~7–8.7 m suggests an intense degree of physicochemical dissolution and corrosion by undersaturated fluids, possibly by sporadic CO_2-charged water in the vadose zone (Loucks, 1999; Cooper and Keller, 2001; Kervin and Woods, 2012). The locally bimodal clast sizes and poor sorting in the granule-sized breccia suggest minor transportation due to flow of vadose water (Kervin and Woods, 2012). The angular breccia with crackle and mosaic fabrics may suggest a shift from phreatic to vadose zone (water table fall), then loss of buoyancy support and roof collapse (Kervin and Woods, 2012).

Grader and Dehler (1999) proposed overall shoreward migration/backstepping of an inner shelf environment during deposition of the lower member of the Jefferson. Overall, the lower member represents a transgressive system tract that is highly diachronous and includes Givetian strata in central Idaho and Frasnian strata in central Wyoming. Our relative sea level curve (Fig. 10) for the Jefferson in Cottonwood Canyon (= lower member of Grader and Dehler, 1999) records high-amplitude, short-term fluctuations in a proximal shallow water environment. At Cottonwood Canyon, the contact between the Maywood Formation and the overlying Jefferson Formation appears gradational, which would suggest a rise in relative sea level and deposition of widespread carbonate.

MADISON LIMESTONE

The Jefferson Formation is unconformably overlain by the Madison Limestone. The lower 3.7 m of the Madison is assigned to the Cottonwood Canyon Member, which includes a 2.7-m-thick lower tongue (upper Middle *expansa* Zone of upper Famennian) and 1-m-thick upper tongue (*S. sandbergi* or *S. duplicata* zones of lower Kinderhookian) with an intervening unconformity (Sandberg and Klapper, 1967). The lower tongue consists of white dolomudstone with a few very thin to thin (<5 cm) interbeds of shale; it is correlative with the lower part of the Sappington Formation in Montana (di Pasquo et al., 2019). The upper tongue is correlative with the Cottonwood Canyon Member of the Lodgepole Formation in Montana (Sandberg and Klapper, 1967; Cole et al., 2015; di Pasquo et al., 2017).

Microfossils

Our sample from the lower tongue of the Cottonwood Canyon Member (Fig. 3) is dominated by large (>100 μm diameter) leiospheres and *Tasmanites*. Subordinate spheroidal forms and other prasinophytes that are less than 100 μm diameter include *Cymatiosphaera rhacoamba*, *Cymatiosphaera perimembrana*, *Stellinium comptum*, *Stellinium micropolygonale*, as well as low diversity acritarchs that include *Dorsennidium polyaster*, *Gorgonisphaeridium elongatum*, *Gorgonisphaeridium plerispinosum*, *Veryhachium lairdi*, and *V. trispinosum* groups (see Sarjeant and Stancliffe, 1994; Stancliffe and Sarjeant, 1994, 1996), *Michrystidium* spp., and rare spores (Fig. 11).

Several authors noted that prior to the early Carboniferous, there were global radiations and diversifications of organic-walled microphytoplankton assemblages (Kroeck et al., 2022), whereas in the early Tournaisian the microplankton experienced a global decline in diversity, referred to as the "Phytoplankton Blackout" (Riegel, 2008), which was marked by the extinction of most acritarchs (Tappan, 1980; Mullins and Servais, 2008; Riegel, 2008) and chitinozoans (Grahn and Paris, 2011). The early Carboniferous assemblages are dominated by morphologically simple, long-ranging genera, such as *Micrhystridium* and *Veryhachium*, and a few prasinophytes. There are few described Devonian–Carboniferous (Mississippian) organic-walled microphytoplankton assemblages from sections with good stratigraphic control. A late Famennian upper Middle *expansa* Zone age for the Cottonwood Canyon Member is supported by the microfossils described herein, with forms that are shared with other Late Devonian and early Carboniferous phytoplankton assemblages (McNestry, 1988; Streel, 1999; Heal and Clayton, 2008; Wicander and Playford, 2013; di Pasquo et al., 2017, 2019; Hogancamp and Pocknall, 2018, and references therein). However, an accurate correlation with spore zonal schemes is difficult because the analyzed sample yielded a scarce and nondiagnostic assemblage of spores. It specifically lacks the diagnostic latest Famennian *Retispora lepidophyta*, perhaps because its parent plant was not present in the region (see di Pasquo et al., 2017, 2019).

CHEMOSTRATIGRAPHY

Maywood and Jefferson Formations

Five carbonate isotope samples were taken from the upper 1.6 m of the Maywood Formation at Cottonwood Canyon (Fig. 10). The $\delta^{13}C_{carb}$ values of the Maywood Formation show a slight negative shift from ~2.5‰ to ~1.7‰. The $\delta^{18}O_{carb}$ ratio rises throughout this entire interval, from −4.9‰ to −1.4‰. The values are clustered around −4‰, suggesting little diagenetic alteration by late-stage meteoric fluids.

There is a shift in $\delta^{13}C_{carb}$ values across the Maywood-Jefferson contact from +1‰ to 2.5‰ to a plateau of ~−0.6‰ (Fig. 10). Above, there is a positive excursion from 8.47 m to 12.67 m that peaks at 1.2‰. This is followed by a negative excursion that begins with an abrupt negative shift to an anomalously low value of ~−5.5‰ at 13.67 m, which is followed by a drift to $\delta^{13}C_{carb}$ values as high as −1.6‰ at 17.6 m below a covered interval (Fig. 10). Initial values above the covered interval are ~−2‰ to −2.4‰, and then they drift negative to −3.6‰ after which they irregularly drift to values of ~0‰ over the 28–34 m interval. The rest of the section has values that vary by ~2‰ around an average of ~0‰ (Fig. 10), although one negative value of −2.2‰ exists at 54.2 m.

Jefferson strata have average $\delta^{18}O_{carb}$ values of ~−4‰ (Fig. 10). No significant excursions in oxygen isotope data are present, although values are more variable between ~24–31 m and ~41–45 m. The overall covariance between $\delta^{13}C_{carb}$ and $\delta^{18}O_{carb}$ is weak (coefficient of determination [R^2] = 0.0251; Fig. 10 inset). The highly vuggy interval from 0.92 m to 8.47 m of the Jefferson shows a moderate level of covariance carbon and oxygen ($R^2 = 0.4103$), suggesting a possible minor degree of diagenetic alteration. The major negative shift in carbon isotopes at 13.67 m does not show a synchronous shift in $\delta^{18}O_{carb}$, suggesting little or no late-stage diagenetic overprint.

In the Logan Canyon section, $\delta^{13}C_{carb}$ values (Fig. 12) in the lower 10.5 m of the Maywood Formation range from ~0.2‰ to 1.1‰, and then shift abruptly negative to ~−0.9‰ at 11.4 m. Above ~12 m is a 3.4 m covered
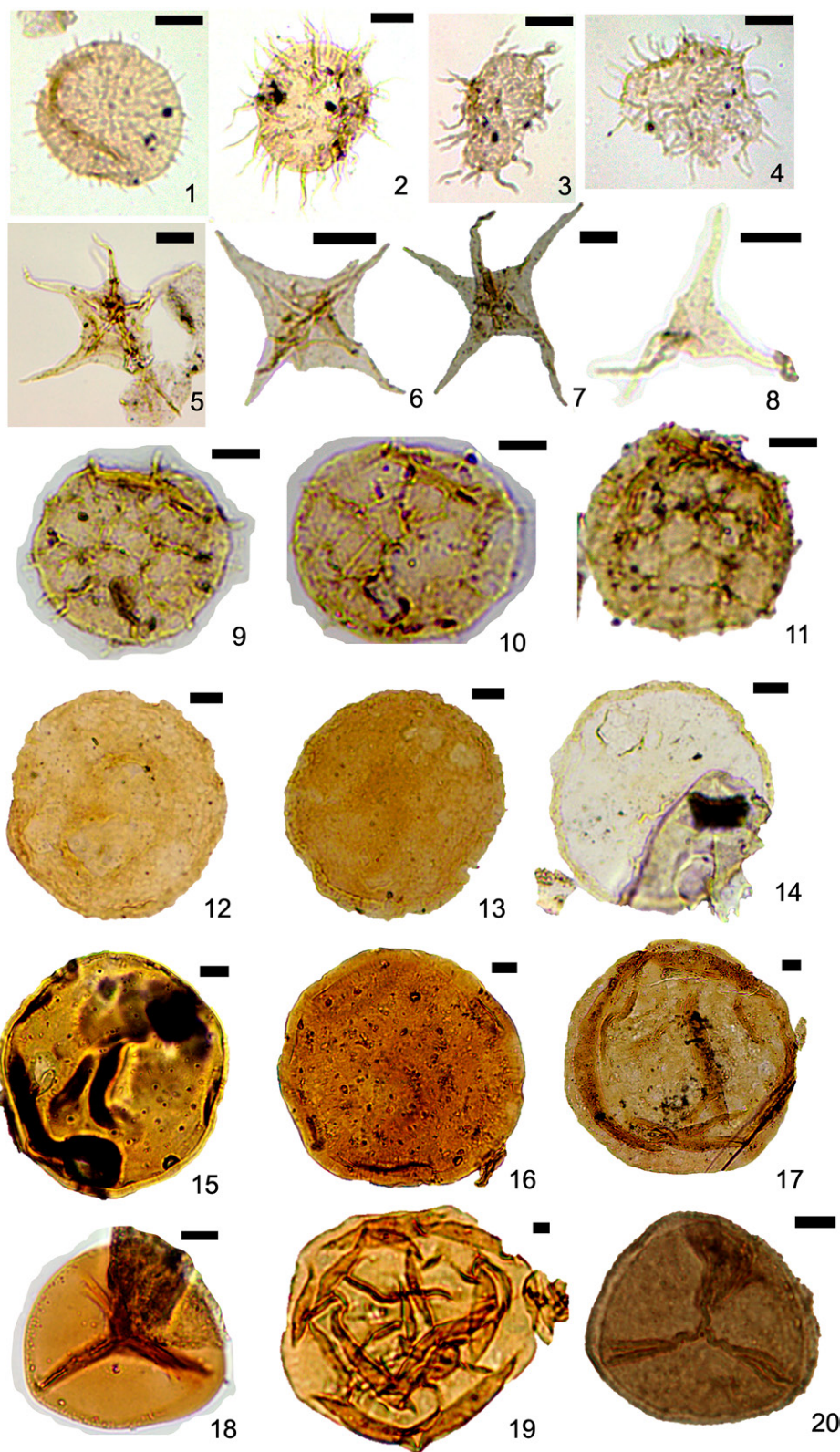
Figure 11. Palynomorphs from the Madison Limestone at Cottonwood Canyon, Wyoming, USA. Sample annotation corresponds to the repository acronym, number, and England Finder coordinates. (1) *Gorgonisphaeridium plerispinosum* Wicander, CICYTTP-Pl 2604(R3818)-C P21/2. (2) *Gorgonisphaeridium ohioense/elongatum* Wicander, CICYTTP-Pl 2604(R3818)-B J17/4. (3) *Michrystridium* sp., CICYTTP-Pl 2604(R3818)-B T36/1. (4) *Michrystridium* sp., CICYTTP-Pl 2604(R3818)-B H18/3. (5) *Stellinium micropolygonale* (Stockman and Willière) Playford, CICYTTP-Pl 2604(R3818)-A M14/3. (6) *Stellinium comptum* Wicander and Loeblich, CICYTTP-Pl 2604(R3818)-B Q13/3. (7) *Dorsennidium polyaster* (Staplin) Sarjeant and Stancliffe, CICYTTP-Pl 2604(R3818)-C Q16/2. (8) *Dorsennidium polyaster* (Staplin) Sarjeant and Stancliffe, CICYTTP-Pl 2604(R3818)-B J18/1. (9) *Cymatiosphaera perimembrana* Staplin, CICYTTP-Pl 2604(R3818)-B G23/4. (10) *Cymatiosphaera rhacoamba* Wicander, CICYTTP-Pl 2604(R3818)-B P17/3. (11) *Cymatiosphaera rhacoamba* Wicander, CICYTTP-Pl 2604(R3818)-B R38/4. (12) *Maranhites* sp., CICYTTP-Pl 2604(R3818)-A E43. (13) *Maranhites* sp., CICYTTP-Pl 2604(R3818)-A E26. (14) *Maranhites* sp., CICYTTP-Pl 2604(R3818)-B F17. (15) *Tasmanites*, CICYTTP-Pl 2604(R3818)-B F17. (16) *Tasmanites*, CICYTTP-Pl 2604(R3818)-B N15/3. (17) *Leiosphaeridia*, CICYTTP-Pl 2604(R3818)-B L15. (18) *Leiotriletes* sp., CICYTTP-Pl 2604(R3818)-B F23/4. (19) *Calamospora* sp., CICYTTP-Pl 2604(R3818)-A V41/2. (20) *Auroraspora* sp., CICYTTP-Pl 2604(R3818)-C V44. Scale bar 10 μm.

interval at the top of the formation, and the initial strata of the Jefferson Formation at 15.6 m record a positive shift to values of ~2.3‰. The next 6.7 m of strata show a steady decline to ~0.2‰. Above a 2.2-m-thick covered zone, there are 2.3 m of strata with a narrow range of values that average ~2.9‰. $\delta^{13}C_{carb}$ values in the strata above an overlying 1.9 m covered interval jump to −1.1‰ and remain consistent for ~3.9 m (up to 31.5 m). There is a highly altered interval with paleokarst breccia directly above, and the lowest overlying sampled strata (at ~33 m) record a dramatic shift to values of ~2‰ (Fig. 12). This is followed by 25 m of section that show a steady drift to values of ~−1.8‰. The next ~13 m show a slow rise to values of ~0.4‰, which includes an anomalous value of ~−2.3‰ at 65.9 m. The next 3.7 m (71.8–75.5 m) show a shift back to values of ~−1‰. This is followed by 4.5 m with a rapid positive shift to values of ~2.8‰ at ~80 m. Above this, the uppermost part of the curve records a positive excursion that peaks at ~0.3‰ (Fig. 12). A cross-plot of $\delta^{13}C_{carb}$ and $\delta^{18}O_{carb}$ values show a determination coefficient of 0.2439, suggesting low probability of significant alteration.

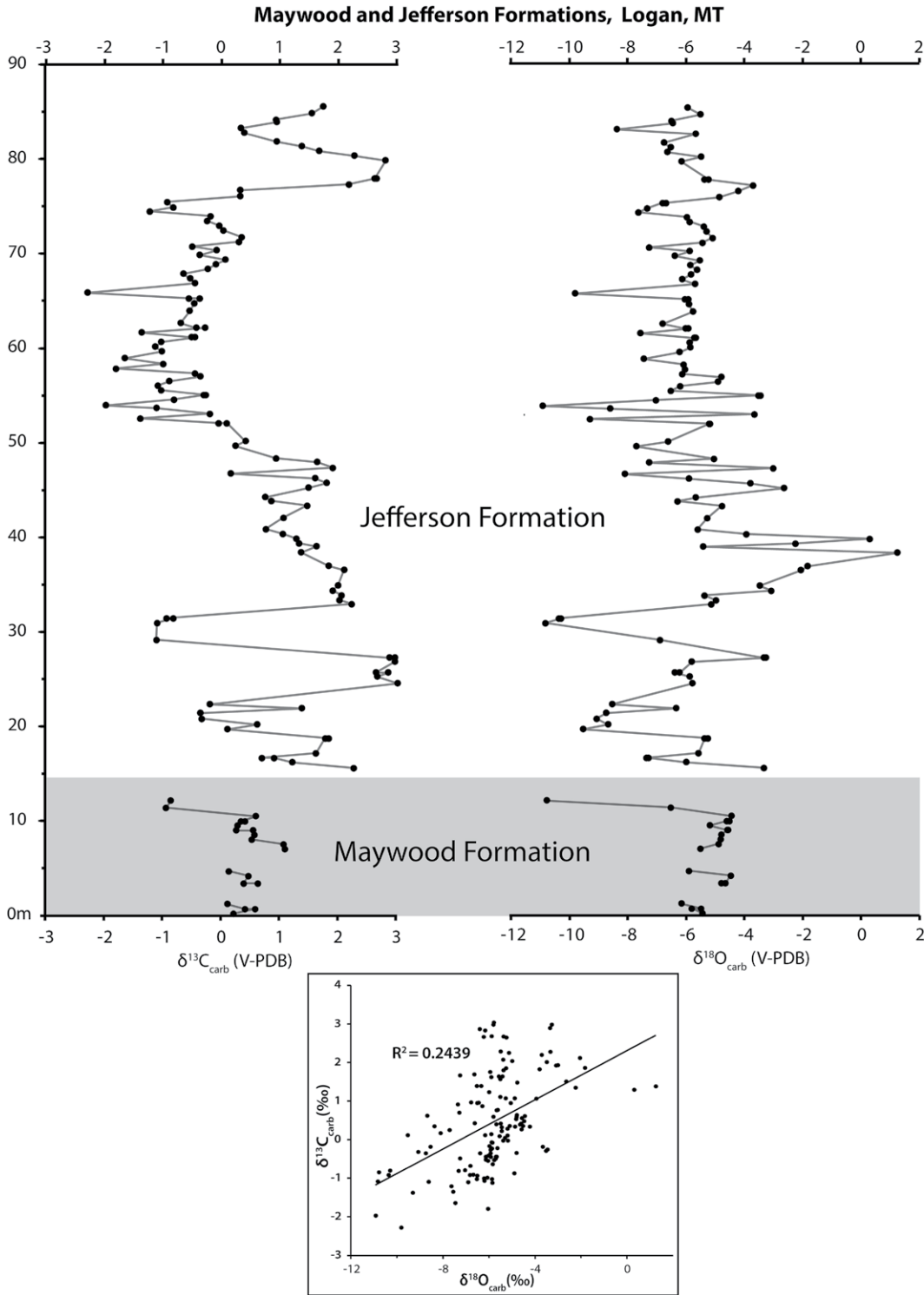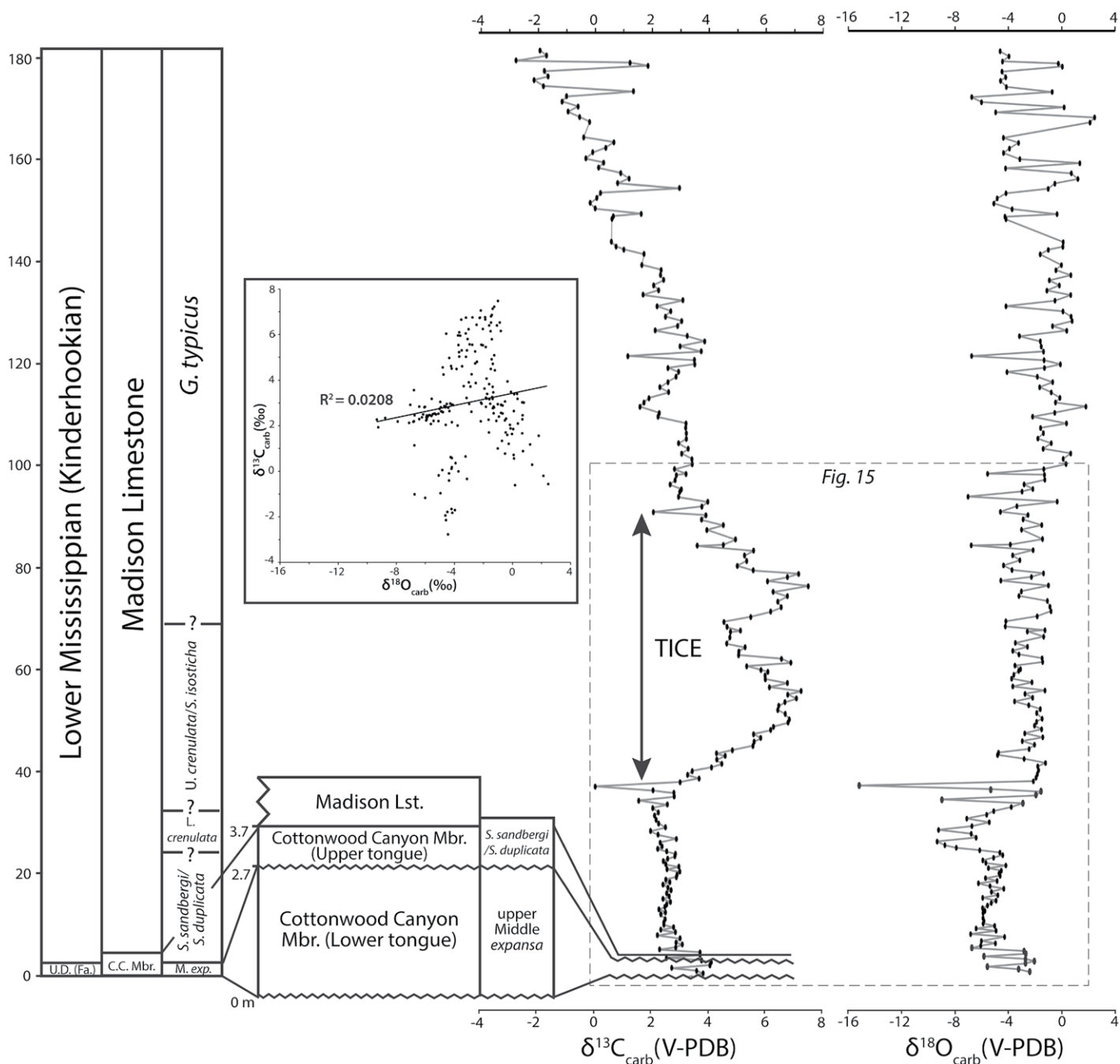**Maywood and Jefferson Formations, Logan, MT**

Figure 12. $\delta^{13}C_{carbonate\ [carb]}$ and $\delta^{18}O_{carb}$ chemostratigraphic data (‰ Vienna Peedee belemnite [V-PDB]) for the Maywood and Jefferson formations at Logan, Montana (MT), USA. Solid line is the best-fit linear regression with coefficient of determination (R^2) = 0.2439.

Madison Limestone

$\delta^{13}C_{carb}$ values for the lower and upper tongues of the Cottonwood Canyon Member (Famennian and lower Kinderhookian, respectively) and lowermost overlying beds oscillate between ~4‰ and 2.4‰ (Fig. 13). These represent a dramatic shift from more negative values of the much older (Frasnian) Jefferson Formation. Above this member, the $\delta^{13}C_{carb}$ values are essentially invariant and average ~2.5‰ up to ~36 m. There is a single low data point at 36.75 m (−0.01‰), which was taken from a heavily weathered and karsted interval. The data between 36.75 m and ~90 m define two $\delta^{13}C_{carb}$ positive excursions within a long-term positive excursion. These smaller excursions peak at ~7‰ at both ~55 m and ~76 m. The data above these excursions record a prolonged negative shift down to approximately −2‰ at the top of the formation (Fig. 13). $\delta^{13}C_{carb}$ data for the upper part of the formation has relatively sharp

Figure 13. Chemostratigraphic data for the Madison Limestone (Lst.) including the Cottonwood Canyon Member (Mbr.), Wyoming, USA (n = 219). $\delta^{13}C_{carbonate\,[carb]}$ and $\delta^{18}O_{carb}$ (‰ Vienna Peedee belemnite [V-PDB]) are plotted against the conodont biostratigraphy on the left, designated based on isotopic correlation. Zigzag lines represent disconformities between the upper and lower tongue of the Cottonwood Canyon Member, and between the lower tongue and the underlying Jefferson Formation. Conodont biostratigraphy of the Cottonwood Canyon Member is after Sandberg and Klapper (1967). Cross plot of $\delta^{13}C_{carb}$ and $\delta^{18}O_{carb}$ is shown in the inset; determination coefficient (R^2) = 0.0208. C.C. Mbr.—Cottonwood Canyon Member; *G. typicus—Gnathodus typicus*; *L. crenulata—Lower crenulata*; *M. exp—Middle expansa*; *S. duplicata—Siphonodella duplicata*; *S. isosticha—Siphonodella isosticha*; *S. sandbergi—Siphonodella sandbergi*; TICE—mid-Tournaisian isotope excursion; *U. crenulata—Upper crenulata*; U.D. (Fa.)—Upper Devonian (Famennian).

variations, particularly in the upper ~30 m. Such high-frequency variation (m-scale variation of a few permil) is unlikely to reflect the global dissolved inorganic carbon (DIC) reservoir.

$\delta^{18}O_{carb}$ data for the Cottonwood Canyon Member at the base of the Madison is highly variable and averages ~3.5‰ (Fig. 13). The overlying $\delta^{18}O_{carb}$ data, up to ~24 m, is relatively

invariant with values of ~−6‰. Values shift negative to ~−9.4‰ at 25.75 m and then rise to ~−3‰ at ~33 m, with a few aberrant points. One anomalously low point of ~−15‰ at

36.75 m, at the base of this interval, corresponds to the negative spike of $\delta^{13}C_{carb}$ curve at the same height. From ~37 m to ~100 m, values show relatively minor oscillation between ~−2‰ and ~−3‰. Above ~100 m, the $\delta^{18}O_{carb}$ values for the rest of the formation average ~−1‰ but include larger amplitude oscillations between ~−7‰ and ~+2.5‰. The entire $\delta^{18}O_{carb}$ dataset of the Madison Limestone averages ~−3‰.

There is strong covariance between the carbon and oxygen isotope values of the lower ~5 m (n = 10) of the section, including both tongues of the 3.7-m-thick Cottonwood Canyon Member (R^2 = 0.9727; see the Supplemental Material [footnote 1]), suggesting substantial strong diagenetic overprint from meteoric fluids. The interval between 33.22 m and 36.75 m, a heavily weathered and karsted interval, might have been similarly affected, as evidenced by a R^2 value of 0.9904 for the carbon and oxygen isotope data (see the Supplemental Material). The remaining data, however, has a low R^2 of 0.0208, suggesting a limited degree of late-stage alteration (see the Supplemental Material). The two positive $\delta^{13}C_{carb}$ excursions between 36.75 m and ~93.5 m correspond to relatively low invariant $\delta^{18}O_{carb}$ values, and thus are considered a primary isotopic signal. Overall, despite evidence for diagenetic alteration in the two mentioned intervals of the section, the rest of the section appears to preserve original $\delta^{13}C_{carb}$ isotopic signatures.

DISCUSSION OF CHEMOSTRATIGRAPHIC DATA

The Late Devonian and early Carboniferous were characterized by a series of repeated, short-term global events that punctuated prolonged periods of relatively stable evolutionary structure (Becker et al., 2016). These events perturbated and re-structured marine and terrestrial ecosystems to different extents, and were similarly marked by transgressive anoxic events, deposition of black shale, and climatic cooling (Algeo et al., 1995; Buggisch and Joachimski, 2006; Qie et al., 2019). These changes have also been linked to global C and S isotope variations. The isotope data of this study are discussed below in the context of such events.

Maywood Formation, Jefferson Formation, and *punctata* Event

At Cottonwood Canyon, the shift from the positive $\delta^{13}C_{carb}$ values of the Maywood Formation (~1.7‰–2.5‰) to the slightly negative values (a plateau of ~−0.4‰ values) in the basal Jefferson (Figs. 12 and 14) is a relatively sharp transition. However, the facies transition appears to be gradational, consistent with a conformable contact, as suggested by Sandberg and McMannis (1964). This negative shift of ~3‰, the shape of the overlying $\delta^{13}C_{carb}$ curve for the rest of the Jefferson Formation, and correlation to sections in northeast Alberta (Holmden et al., 2006), provide the first definitive age of the Maywood as lowermost Frasnian, within the middle *falsiovalis* conodont zone (Fig. 14). This supports Marshall et al.'s (2022) suggestion that the depauperate palynoflora of the Maywood solely reflects stressed paleoenvironmental conditions, consistent with recent reconstructions of the habitat (Zatoń et al., 2022; di Pasquo et al., 2022), rather than an uppermost Givetian age.

Maywood Formation strata exposed close to Logan, Montana, at Milligan Canyon yielded the conodont *Pandorinellina insita* and the brachiopod *Allanella allani* (Sandberg et al., 1988). The former ranges from uppermost Givetian to uppermost *punctata* Zone of Frasnian (Klapper, 1977). The brachiopod *A. allani* ranges from uppermost Givetian to the base of the *punctata* Zone (Jed Day, pers. comm., 2022). Thus, the existing biostratigraphic data lacks fine-scale resolution. However, our chemostratigraphic data allows for precise correlation of the Logan and Cottonwood Canyon sections. The Maywood data at Logan do not include any positive values (~+2‰), as present in Cottonwood Canyon, and instead have only very slightly positive values. Based on our correlations (Fig. 14), the Maywood at Logan is assignable to the upper *transitans* Zone and is thus equivalent to the lower to middle Jefferson Formation at Cottonwood Canyon. Hence, the nearshore strata of the Maywood Formation at Logan are much younger than the Maywood at Cottonwood Canyon (middle *falsiovalis* Zone), and therefore the formation is significantly diachronous: older in northern Wyoming and younger in southern Montana (Fig. 14). This time transgression suggests that the southern Montana sections would have been topographically higher than the northern Wyoming sections during transgression, and that there was delayed onlap of the Maywood Formation. The Montana sections rest on Cambrian strata, indicating that a considerably thick Ordovician Bighorn Dolostone was completely eroded in this area, supporting the idea that this region was uplifted and was subjected to greater erosion down to lower stratigraphic levels. This is supported by isopach maps showing that Ordovician strata are missing from west-central Montana and that strata of this age thicken to the west toward the longitude of the Bighorn Mountains (Foster, 1972). Isotopic data for the lower part of the Jefferson Formation at Cottonwood Canyon show significant positive and negative excursions, most of which are in strata that have no evidence for subaerial exposure, peritidal facies, or low $\delta^{18}O_{carb}$ values. There is a major positive excursion in $\delta^{13}C_{carb}$ values between 8.72 m and 12.67 m, and a subsequent negative excursion between 12.67 m and 17.64 m (with a single value of ~−5.5‰; Fig. 14). These data are interpreted to represent a signal of the *punctata* Event, one of several major Frasnian events (Sandberg et al., 2002; Qie et al., 2011; Becker et al., 2016). The event is defined, in part, by a paired positive and negative isotopic excursion within the lower part of the Frasnian *punctata* Zone interval (Yans et al., 2007; Pisarzowska and Racki, 2012; Lash, 2019; Pisarzowska et al., 2020; Fig. 14). The Jefferson *punctata* Zone positive excursion at Cottonwood Canyon begins above a sandstone bed at 8.72 m, with a thick paleokarst and fenestrae-rich horizon below, and thus it also records transgression above a subaerial exposure surface (= sequence boundary) (Fig. 10). This exposure surface likely explains the high covariance between $\delta^{13}C_{carb}$ and $\delta^{18}O_{carb}$ values of the interval below. There are no major facies changes in the interval of the positive and negative excursions.

The lower part of the Jefferson Formation at Logan records a more variable, but recognizable, *punctata* positive excursion in $\delta^{13}C_{carb}$ between ~12 m and 31.5 m (Fig. 12). The negative values (~−1.1‰) at the top of this excursion mark the nadir of the negative *punctata* Event excursion, which is well expressed in the middle part of Jefferson at Cottonwood Canyon (this study) and in sections globally (Fig. 14). A rapid positive shift, and subsequent long-term overlying drift toward negative values, is very well matched with a NE Alberta section (Holmden et al., 2006; Fig. 14). A few variable and negative $\delta^{13}C_{carb}$ values in the lower half of the Logan section are associated with highly negative $\delta^{18}O_{carb}$ values, but not all, and the overall shapes of the curves in the NE Alberta section, Cottonwood Canyon, and Logan sections (Fig. 14) indicate that a primary signal is preserved at Logan despite many petroliferous intervals.

Significance of the *punctata* Event

The *punctata* Event is suggested to be global in nature as it is recognized in Europe, Siberia, China, and North America (Holmden et al., 2006; Yans et al., 2007; Morrow et al., 2009; Śliwiński et al., 2011; Pisarzowska and Racki, 2012, 2020; Pisarzowska et al., 2020). The entire *punctata* Event is considered to have been an abrupt global perturbation in the carbon cycle that lasted less than 1.5 million years (Pisarzowska et al., 2006; Yans et al., 2007; Racki et al., 2008). The positive excursion (average ~4‰–5‰) of the event began close to the *transitans–punctata* zonal bound-
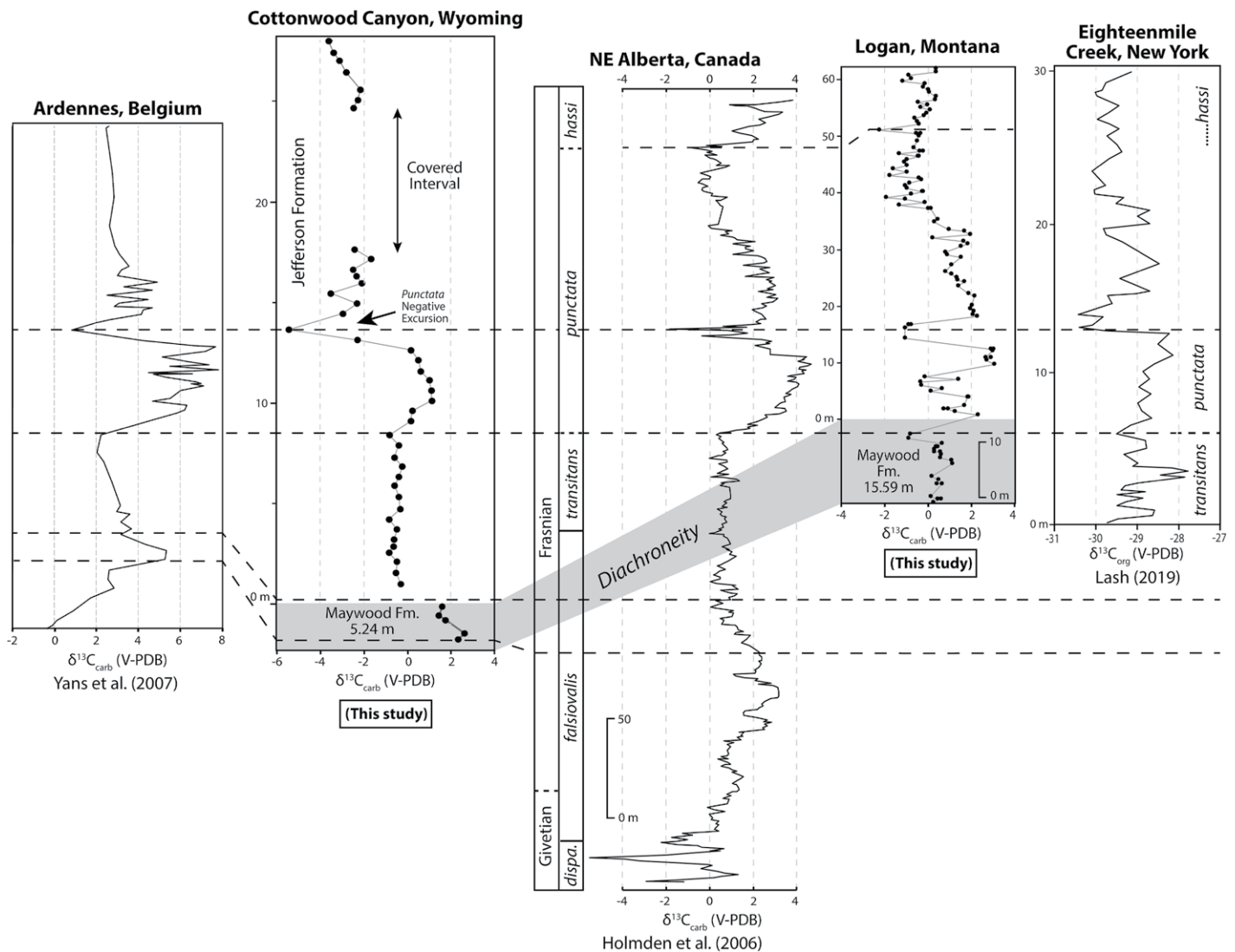
Figure 14. Correlations of δ¹³C_carbonate [carb] data from Maywood and Jefferson formations at Cottonwood Canyon, Wyoming, and Logan, Montana, USA, with published data for strata of similar ages. The data of Lash (2019) is δ¹³C_organic [org] (‰ Vienna Peedee belemnite [V-PDB]) from shale. The shaded band indicates a diachroneity of the Maywood Formation (Fm.) between the Cottonwood Canyon section and the Logan section (see text). *dispa.—disparilis*.

ary (Johnson et al., 1985), although estimates of the exact timing and magnitude are variable (Śliwiński et al., 2011; Pisarzowska and Racki, 2012; Lash, 2019). The positive excursion is correlated to the IIc transgression, which corresponds to the Middlesex transgressive anoxic event (Morrow et al., 2009; Pisarzowska and Racki, 2012; Pisarzowska et al., 2020). Proposed causes for the positive isotopic excursion include heightened detritus delivery due to orogenic uplift and terrestrial afforestation (Algeo et al., 1995; Nawrocki et al., 2008; Meyer-Berthaud et al., 2010; Śliwiński et al., 2011), and bottom water anoxia and euxinia (Racki et al., 2008; Śliwiński et al., 2011; Pisarzowska and Racki, 2012). Enhanced organic carbon burial and preservation is supported by abundant

organic-rich deposits in Lower to Middle Frasnian successions (see Morrow et al., 2009).

The abrupt negative excursion of the *punctata* Event (Fig. 14) was possibly a result of the Alamo Impact in southern Nevada (Yans et al., 2007), which occurred <650 k.y. after the *punctata–transitans* zonal boundary (Morrow et al., 2009). This was a marine impact of an extraterrestrial bolide that produced thick tsunami deposits, shocked-quartz grains, anomalously high iridium levels, and lapilli ejecta (Warme and Sandberg, 1995; Sandberg et al., 1997). Similar impact features (spherules and lapilli) have been reported from eastern Laurentia (Lash, 2019) and Czech Republic (Hladil et al., 2009). The duration of the negative δ¹³C_carb excursion is estimated to be ~13–30 k.y. (Lash, 2019), and thus it may

reflect the rapid release of substantial seafloor methane hydrates triggered by the impact (Yans et al., 2007; Lash, 2019). Alternative hypotheses for the negative excursion include (1) a decrease in primary productivity related to a eustatic lowstand (Pisarzowska and Racki, 2012) and (2) volcanic activity connected with Devonian large igneous provinces and arc magmatism (Pisarzowska et al., 2020; Racki, 2020).

Madison Limestone and the Mid-Tournaisian/Kinderhookian–Osagean Boundary Carbon Isotope Excursion (TICE/KOBE) Event

The highly variable δ¹³C_carb values at the base of the Madison Limestone, in the lower and upper

tongues of the Cottonwood Canyon Member, contrast with the more invariant values (~2.5‰) directly above (Fig. 13). We attribute this variability to diagenetic alteration, which may, in part, be related to the unconformity between the two tongues of the member (Sandberg and Klapper, 1967). The Madison Limestone data from Cottonwood Canyon, Wyoming, record a long-term positive excursion between 36.75 m and 90.5 m, which consists of two peaks, both of which have peak values of ~+7‰ (Figs. 13).

We interpret the large positive excursion in the Madison to represent the Kinderhookian–Osagean boundary excursion (KOBE), also known as the mid-Tournaisian isotope excursion (TICE). It is identified from upper Kinderhookian to lower Osagean strata (*Siphonodella isosticha*–Upper *S. crenulata* to *Gnathodus typicus* conodont zones, lasting ~2–3 m.y.) (Saltzman, 2003; Buggisch et al., 2008; Yao et al., 2015) (Fig. 15). This $\delta^{13}C_{carb}$ isotope excursion (up to +7.3‰) is one of the highest in the Phanerozoic and is commonly associated with a positive shift of conodont and brachiopod $\delta^{18}O$ (Mii et al., 1999; Buggisch et al., 2008). TICE/KOBE is recorded in the western United States, and similar signatures are documented globally (Mii et al., 1999; Saltzman, 2002, 2003; Buggisch et al., 2008; Qie et al., 2011). It typically consists of two smaller positive peaks within a long-term positive excursion, like our Madison data (Fig. 15), although not all documented sections show such double-peak patterns. Saltzman (2003) recognized similar isotopic signals from roughly age-equivalent strata with paired positive excursions that peak at ~6‰. An ~6‰ positive excursion in $\delta^{13}C_{carb}$ is present at Sacajewea Peak, Montana, within the Lodgepole Limestone, the majority of which is dated Upper *crenulata* to *S. isosticha* Zone (Sandberg and Klapper, 1967; Cole et al., 2015). The second peak of TICE/KOBE is recorded within lower *G. typicus* conodont zone strata (Fig. 15).

The lower Carboniferous corresponds to a transition from Devonian greenhouse to Carbon-
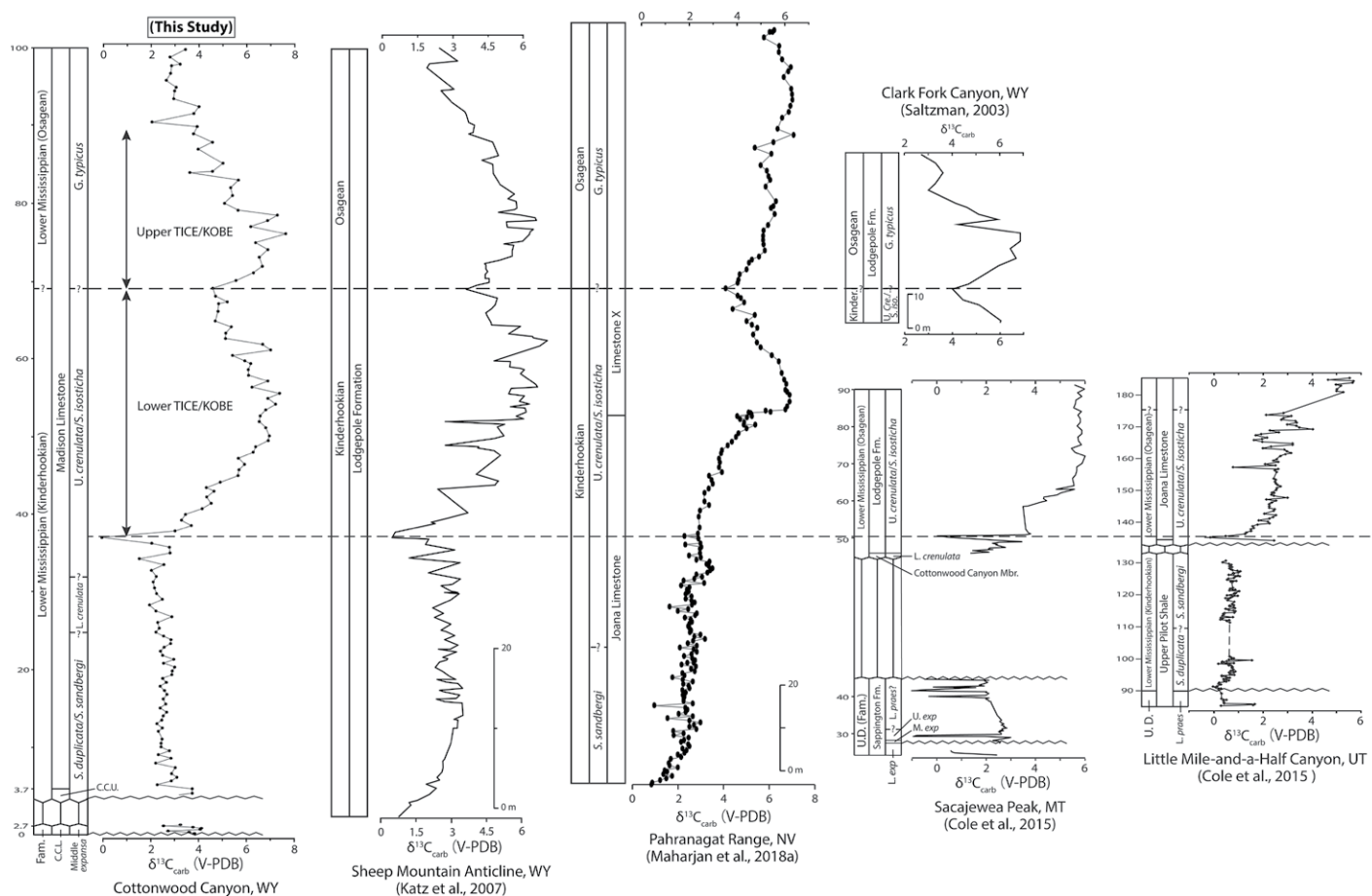
Figure 15. Correlations of $\delta^{13}C_{carbonate\ [carb]}$ (‰ **Vienna Peedee belemnite [V-PDB]**) **data from Madison Limestone at Cottonwood Canyon, Wyoming (WY), USA, with published data for strata of similar ages. Sections with conodont biostratigraphy constraints are indicated on the left of respective curve, in which solid lines represent well-defined boundaries and dashed lines indicate inferred boundaries. Horizontal zigzag lines indicate unconformities. Black dashed lines represent isotopic correlations. The mid-Tournaisian/Kinderhookian–Osagean boundary carbon isotope excursion (TICE/KOBE) event consists of two smaller positive excursions within a long-term positive excursion. The first positive excursion starts in the lower part of Upper (U.) *crenulata* / *Siphonodella* (*S.*) *isosticha* (lower dashed line) and ends at the Kinderhookian–Osagean boundary (middle dashed line). The upper dashed line represents the peak of the second excursion in *Gnathodus* (*G.*) *typicus*. C.C.L—lower tongue of the Cottonwood Canyon Member; C.C.U—upper tongue of the Cottonwood Canyon Member; Fam.—Famennian; Fm.—Formation; L. *exp.*—Lower *expansa*; L. *praes.*—Lower *praesulcata*; Mbr.—Member; M. *exp*—Middle *expansa*; MT—Montana (USA); NV—Nevada (USA); *S. iso.*—*Siphonodella isosticha*; U. *cre.*—Upper *crenulata*; U. *exp.*—Upper *expansa*; U.D.—Upper Devonian; UT—Utah (USA).**

iferous–Permian icehouse conditions, caused in part by an atmospheric pCO_2 level drop from >10 present atmospheric level to ∼pre-industrial level of ∼280 ppm (Berner, 2006; Buggisch et al., 2008; Foster et al., 2017; Qie et al., 2019). The lower Carboniferous transition followed the Frasnian temperature maximum and a transient cooling event that took place during the Frasnian–Famennian boundary interval, all of which was followed by climatic cooling during most of the Famennian (Joachimski et al., 2004; Buggisch et al., 2008; Huang et al., 2018; Girard et al., 2020). Sedimentological and geochemical records suggest a global climatic cooling, expansion of continental ice volume, and a major regression during the TICE/KOBE interval (Bruckschen et al., 1995; Mii et al., 1999; Buggisch et al., 2008; Caputo et al., 2008; Kammer and Matchen, 2008; Bishop et al., 2009). The positive excursion in the late Kinderhookian and early Osagean has been interpreted to represent enhanced productivity and organic carbon burial due to increased nutrient delivery to surface water from the continents or from the deeper ocean by upwelling, although [87]Sr data suggest low weathering fluxes during this time (Bruckschen et al., 1995; Kump and Arthur, 1999; Mii et al., 1999). This is supported by upper *G. typicus* Zone phosphorite deposits in the Antler foreland TICE/KOBE successions that are thought to represent high organic carbon burial and phosphate enrichment during *S. isosticha*, under a stratified hypoxic water column (Saltzman, 2003). Widespread ocean anoxia has also been proposed based on $\delta^{238}U$ and $\delta^{34}S$ data, and this might have led to enhanced preservation of organic carbon (Maharjan et al., 2018b; Cheng et al., 2020). Cheng et al. (2020) suggested that the first peak in $\delta^{13}C$ of the TICE/KOBE resulted from euxinic seafloor conditions (see Maharjan et al., 2018b), which was followed by anoxic/suboxic conditions that correlate to the second spike. $\delta^{34}S$ data from both pyrite ($\delta^{34}S_{pyrite}$) and carbonate-associated sulfate ($\delta^{34}S_{CAS}$) demonstrate an expansion of oxygen minimum zone (OMZ) with maximum sulfate reduction and pyrite burial concurrent with the first peak in $\delta^{13}C$. The expansion of OMZ and sulfate reduction would add ^{13}C-depleted organic matter back to the DIC and produced the small negative shift in $\delta^{13}C$ (Maharjan et al., 2018b). Many studies suggest that upwelling due to intensified thermohaline circulation, possibly related to climatic cooling, may intensify anoxia within the OMZ and shift the locus of denitrification, eventually stimulating primary production in the surface water (Buggisch et al., 2008; Maharjan et al., 2018a; Liu et al., 2019). Spatial variations of the magnitude of the $\delta^{13}C$ excursion are proposed to result from differences in circulation strength and marine nutrient concentration (Liu et al., 2019; Saltzman, 2003).

Proliferation of vascular plants and associated contribution to marine productivity is proposed by some authors to account for this positive carbon isotope excursion (e.g., Berner and Barron, 1984; Algeo et al., 1995). However, it will be difficult to resolve several cooling and marine anoxia events prior to the TICE/KOBE based on their theory (Kabanov, 2021), although the evolving plants could amplify the drawdown of pCO_2 in the lower Carboniferous climate transition. Many recent studies suggest that the climatic cooling was ultimately tectonic driven and related to the closure of the Rheic Ocean as Pangea was forming (Veevers and Powell, 1987; Woodward et al., 2013; Qiao and Shen, 2014; Goddéris et al., 2017; Liu et al., 2019). The ongoing closure of the Rheic Ocean limited equatorial ocean currents, altering the thermohaline circulation and promoted the growth of Gondwana glaciation. TICE/KOBE may have thus been associated with a major step of volume increase of Gondwana ice sheets and the expansion of the late Paleozoic icehouse climate (Yao et al., 2015; Goddéris et al., 2017; Liu et al., 2019).

PALEOGEOGRAPHY

The combination of palynological and chemostratigraphic data presented herein have important implications for paleogeographic reconstructions. Sandberg (1963) suggested an early Frasnian age for the Maywood strata at Cottonwood Canyon based on the plant and fish fossils, without mention of specific biozones of the Frasnian. Morrow et al. (2005) suggested that the carbonized plant material of the Maywood at that section may record wildfires produced by the Frasnian (*punctata* Zone) Alamo Breccia impact event. However, our chemostratigraphic data record the *punctata* Event excursion ∼9–18 m above the base of the overlying Jefferson Formation (Fig. 14), and thus the Maywood is too old at this site to record the Alamo impact event. Our chemostratigraphic data indicate an uppermost *transitans* to lowermost *punctata* Zone age for the Maywood for exposures in the Three Forks area in Montana (including the Logan section). Sandberg et al. (1988) reported middle *asymmetrica* Zone conodonts (middle Frasnian = *punctata* Zone) from the uppermost Maywood there, and the *punctata* Event excursion is in the lowermost Jefferson in that section. Using the transgressive-regressive cycle terminology for western North America presented by Johnson and Sandberg (1988) and modified by Day et al. (1996) and LaMaskin and Elrick (1997), the Maywood Formation at Cottonwood

Canyon would have been deposited early in the IIb cycle, following the Givetian Taghanic event (IIa transgressive-regressive cycle).

Sandberg (1961b, 1963) suggested that the Maywood Formation (= Souris River Formation) at Cottonwood Canyon was deposited in the upper reaches of long, narrow estuaries that extended into the paleoshorelines of the Williston Basin seaway (= Souris River seaway) to the northwest (Sandberg, 1963). Sandberg and McMannis (1964) presented a more regional view of the paleogeography by which the Maywood Sea, an arm of the Cordilleran seaway, transgressed eastward and merged in central Montana with the Williston Basin seaway, which had transgressed westward. In their view, the merged sea then transgressed from north to south, such that the Gallatin Range section (Fig. 6) would have been the upstream estuarine equivalent of the other southern Montana sections, e.g., Logan and Milligan Canyon, the latter with marine fossils, in the same way that the Cottonwood Canyon section would have been the upper estuarine reaches of the Williston Basin (or merged) seaway. This is consistent with relationships we observed *within* southern Montana; namely, that the Gallatin Range section (Fig. 6) has a clearly channelized geometry and more abundant siliciclastic detritus relative to the Logan and Milligan Canyon, Montana, sections to the north. However, although the Maywood in these latter locations is thicker, and at Milligan Canyon it bears marine brachiopods and conodonts at the top of the formation (Sandberg et al., 1988), the revised older age of the Maywood at Cottonwood Canyon requires that the proposed reconstruction be altered. The Cottonwood Canyon section records a transgressive succession from restricted nearshore/estuarine Maywood environments to open marine, widespread carbonate deposition of the Jefferson, which took place within the *falsiovalis* Zone of the lowermost Frasnian. The southern Montana sections record a similar shift, but it occurs later, *within* the lower part of the *punctata* Zone. This indicates significant diachroneity of the Maywood Formation (Fig. 14) and either marine transgression from south to north, with open marine environment established in northern Wyoming prior to southern Montana, or a much more complicated regional paleogeography, particularly as some Maywood strata in Montana are much older.

CONCLUSIONS

$\delta^{13}C_{carb}$ and $\delta^{18}O_{carb}$ chemostratigraphic, paleontological, physical stratigraphic, and relative sea level data of Devonian–lower Carboniferous (Tournaisian) strata has allowed a thor-

ough reconstruction of the dynamic evolution of Devonian paleogeography in the northern U.S. Rocky Mountain region. The Maywood Formation at Cottonwood Canyon, Wyoming, records infilling of a valley that was cut into both the upper Beartooth Butte Formation and Bighorn Dolomite. A palynological analysis of microspores from the formation suggest a shallow, brackish environment. The lithofacies and unusual low-diversity assemblage of microconchids and fish debris mimics those from a much older Beartooth Butte Formation valley filling deposits. This indicates that over a span of nearly 30 m.y. of the Early to Late Devonian, there was a repeated pattern of valley incision and subsequent transgression, with the migration of a salinity-stressed faunal assemblage that tracked transgressions. This is a remarkable and unusual paleogeographic and paleoecologic pattern of the middle to late Paleozoic depositional history of the northern Rocky Mountains. General tectonic quiescence during this interval implies that eustasy or uplift associated with dynamic topography (mantle flow) was likely the driving force of these repeated events of valley incision and deposition. The widespread plant fossils present in these strata are a partial record of a global interval of increase in the size and abundance of woody shrubs in terrestrial environments. Abundant charcoal in the Maywood marks the impact of fire on the landscape during the evolution of terrestrial ecosystems, providing a useful global constraint on atmospheric O_2 concentrations during the earliest part of the Late Devonian (>16% by volume). Marine transgression resulted in the transition from nearshore/estuarine deposition to extensive low-energy, shallow, carbonate shelf deposition of the Frasnian Jefferson Formation limestone.

Chemostratigraphic correlations indicate that Maywood Formation of the Three Forks area of southern Montana is *transitans* to lowermost *punctata* Zone in age, revealing considerable diachroneity of the formation and an opposite polarity (S-N) of the previously suggested direction of transgression (N-S). The pattern is also inconsistent with the idea that the Maywood at Cottonwood Canyon represents the upper reaches of estuaries that extended from a seaway in southern Montana.

$\delta^{13}C_{carb}$ data for the Jefferson Formation at Cottonwood Canyon record a paired positive and negative excursion of the middle Frasnian (*punctata* Zone). The Jefferson Formation is unconformably overlain by the Madison Limestone, including a thin basal Cottonwood Canyon Member (latest Devonian to earliest lower Carboniferous) that has yielded a diverse suite of organic-walled microphytoplankton fossils, which predate the early lower Carboniferous

microplankton extinction. $\delta^{13}C_{carb}$ isotope data demonstrate two peaks within a long-term positive excursion, which correlates to the global TICE/KOBE event from Kinderhookian to Osagean. This excursion is suggested to be caused by enhanced primary production and burial of organic carbon and is concurrent with climatic cooling and widespread ocean anoxia event.

REFERENCES CITED

Aboussalam, Z.S., 2003, Das "Taghanic-Event" im höheren Mittel-Devon von West-Europa und Marokko: Münstersche Forschungen zur Geologie und Paläontologie, v. 97, 332 p.

Aboussalam, Z.S., and Becker, R.T., 2011, The global Taghanic Biocrisis (Givetian) in the eastern Anti-Atlas, Morocco: Palaeogeography, Palaeoclimatology, Palaeoecology, v. 304, p. 136–164, https://doi.org/10.1016/j.palaeo.2010.10.015.

Algeo, T.J., and Ingall, E., 2007, Sedimentary C_{org}: P ratios, paleocean ventilation, and Phanerozoic atmospheric pO_2: Palaeogeography, Palaeoclimatology, Palaeoecology, v. 256, p. 130–155, https://doi.org/10.1016/j.palaeo.2007.02.029.

Algeo, T.J., and Scheckler, S.E., 1998, Terrestrial–marine teleconnections in the Devonian: Links between the evolution of land plants, weathering processes, and marine anoxic events: Philosophical Transactions of the Royal Society of London B: Biological Sciences, v. 353, p. 113–130, https://doi.org/10.1098/rstb.1998.0195.

Algeo, T.J., Berner, R.A., Maynard, J.B., and Scheckler, S.E., 1995, Late Devonian oceanic anoxic events and biotic crises: "rooted in the evolution of vascular land plants?": GSA Today, v. 5, p. 64–66.

Beck, C.B., 1966, On the origin of gymnosperms: Taxon, v. 15, p. 337–339, https://doi.org/10.2307/1217162.

Becker, R.T., Königshof, P., and Brett, C.E., 2016, Devonian climate, sea level and evolutionary events: An introduction, *in* Becker, R.T., Königshof, P., and Brett, C.E., eds., Devonian Climate, Sea Level and Evolutionary Events: Geological Society, London, Special Publication 423, p. 1–10, https://doi.org/10.1144/SP423.15.

Belcher, C.M., Yearsley, J.M., Hadden, R.M., McElwain, J.C., and Rein, G., 2010, Baseline intrinsic flammability of Earth's ecosystems estimated from paleoatmospheric oxygen over the past 350 million years: Proceedings of the National Academy of Sciences of the United States of America, v. 107, p. 22,448–22,453, https://doi.org/10.1073/pnas.1011974107.

Belcher, C.M., Collinson, M.E., and Scott, A.C., 2013, A 450-million-year history of fire: Fire phenomena and the Earth system: An interdisciplinary guide to fire science, *in* Belcher, C.M., ed., Fire Phenomena and the Earth System: Hoboken, New Jersey, USA, Wiley-Blackwell, p. 207–227, https://doi.org/10.1002/9781118529539.

Benson, A.L., 1966, Devonian stratigraphy of western Wyoming and adjacent areas: American Association of Petroleum Geologists Bulletin, v. 50, p. 2566–2603.

Berner, R.A., 2006, GEOCARBSULF: A combined model for Phanerozoic atmospheric O_2 and CO_2: Geochimica et Cosmochimica Acta, v. 70, p. 5653–5664, https://doi.org/10.1016/j.gca.2005.11.032.

Berner, R.A., and Barron, E.J., 1984, Comments on the BLAG model: Factors affecting atmospheric CO_2 and temperature over the past 100 million years: American Journal of Science, v. 284, p. 1183–1192, https://doi.org/10.2475/ajs.284.10.1183.

Berner, R.A., and Raiswell, R., 1983, Burial of organic carbon and pyrite sulfur in sediments over Phanerozoic time: A new theory: Geochimica et Cosmochimica Acta, v. 47, p. 855–862, https://doi.org/10.1016/0016-7037(83)90151-5.

Bishop, J.W., Montañez, I.P., Gulbranson, E.L., and Brenckle, P.L., 2009, The onset of mid-Carboniferous glacioeustasy: Sedimentologic and diagenetic constraints, Arrow Canyon, Nevada: Palaeogeography, Palaeoclimatology, Palaeoecology, v. 276, p. 217–243, https://doi.org/10.1016/j.palaeo.2009.02.019.

Bowman, D.M.J.S., et al., 2009, Fire in the Earth system: Science, v. 324, p. 481–484, https://doi.org/10.1126/science.1163886.

Bruckschen, P., Bruhn, F., Veizer, J., and Buhl, D., 1995, $^{87}Sr/^{86}Sr$ isotopic evolution of Lower Carboniferous seawater: Dinantian of western Europe: Sedimentary Geology, v. 100, p. 63–81, https://doi.org/10.1016/0037-0738(95)00103-4.

Buggisch, W., and Joachimski, M., 2006, Carbon isotope stratigraphy of the Devonian of Central and Southern Europe: Palaeogeography, Palaeoclimatology, Palaeoecology, v. 240, p. 68–88, https://doi.org/10.1016/j.palaeo.2006.03.046.

Buggisch, W., Joachimski, M.M., Sevastopulo, G., and Morrow, J.R., 2008, Mississippian $\delta^{13}C$ and conodont apatite $\delta^{18}O$ records: Their relation to the Late Palaeozoic Glaciation: Palaeogeography, Palaeoclimatology, Palaeoecology, v. 268, p. 273–292, https://doi.org/10.1016/j.palaeo.2008.03.043.

Burbank, D.W., Leland, J., Fielding, E., Anderson, R.S., Brozovic, N., Reid, M.R., and Duncan, C., 1996, Bedrock incision, rock uplift and threshold hillslopes in the northwestern Himalayas: Nature, v. 379, p. 505–510, https://doi.org/10.1038/379505a0.

Canter, K.L., Wheeler, D.M., and Geesaman, R.C., 1992, Sequence stratigraphy and depositional facies of the Siluro-Devonian interval of the northern Permian Basin, *in* Candelaria, M.P., and Reed, C.L., eds, Paleokarst, Karst-Related Diagenesis, and Reservoir Development: Examples from Ordovician–Devonian Age Strata of West Texas and the Mid-Continent: Permian Basin Section, SEPM (Society for Sedimentary Geology), Field Trip Guidebook, v. 92-33, p. 93–109.

Cao, W., Flament, N., Zahirovic, S., Williams, S., and Müller, R.D., 2019, The interplay of dynamic topography and eustasy on continental flooding in the late Paleozoic: Tectonophysics, v. 761, p. 108–121, https://doi.org/10.1016/j.tecto.2019.04.018.

Caplan, M.L., and Bustin, M.R., 1999, Devonian–Carboniferous Hangenberg mass extinction event, widespread organic-rich mudrock and anoxia: Causes and consequences: Palaeogeography, Palaeoclimatology, Palaeoecology, v. 148, p. 187–207, https://doi.org/10.1016/S0031-0182(98)00218-1.

Caputo, M.V., Melo, J.H.G., Streel, M., and Isbell, J.L., 2008, Late Devonian and Early Carboniferous glacial records of South America, *in* Fielding, C.R., Frank, T.D., and Isbell, J.L., eds., Resolving the Late Paleozoic Ice Age in Time and Space: Geological Society of America Special Paper 441, p. 161–173, https://doi.org/10.1130/2008.2441(11).

Caruso, J.A., and Tomescu, A.M., 2012, Microconchid encrusters colonizing land plants: The earliest North American record from the Early Devonian of Wyoming, USA: Lethaia, v. 45, p. 490–494, https://doi.org/10.1111/j.1502-3931.2012.00305.x.

Chaloner, W.G., 1989, Fossil charcoal as an indicator of palaeo-atmospheric oxygen level: Journal of the Geological Society, v. 146, p. 171–174, https://doi.org/10.1144/gsjgs.146.1.0171.

Cheng, K., Elrick, M., and Romaniello, S.J., 2020, Early Mississippian ocean anoxia triggered organic carbon burial and late Paleozoic cooling: Evidence from uranium isotopes recorded in marine limestone: Geology, v. 48, p. 363–367, https://doi.org/10.1130/G46950.1.

Cohen, K.M., Finney, S.C., Gibbard, P.L., and Fan, J.-X., 2013, The ICS International Chronostratigraphic Chart: Episodes, v. 36, p. 199–204, https://doi.org/10.18814/epiiugs/2013/v36i3/002.

Cole, D., Myrow, P.M., Fike, D.A., Hakim, A., and Gehrels, G.E., 2015, Uppermost Devonian (Famennian)

to Lower Mississippian events of the western U.S.: Stratigraphy, sedimentology, chemostratigraphy, and detrital zircon geochronology: Palaeogeography, Palaeoclimatology, Palaeoecology, v. 427, p. 1–19, https://doi.org/10.1016/j.palaeo.2015.03.014.

Cooper, J.D., and Keller, M., 2001, Palaeokarst in the Ordovician of the southern Great Basin, USA: Implications for sea-level history: Sedimentology, v. 48, p. 855–873, https://doi.org/10.1046/j.1365-3091.2001.00393.x.

Cope, M.J., and Chaloner, W.G., 1980, Fossil charcoal as evidence of past atmospheric composition: Nature, v. 283, p. 647–649, https://doi.org/10.1038/283647a0.

Cressler, W.L., III, 2001, Evidence of earliest known wildfires: Palaios, v. 16, p. 171–174, https://doi.org/10.1669/0883-1351(2001)016<0171:EOEKW>2.0.CO;2.

Dahl, T.W., Hammarlund, E.U., Anbar, A.D., Bond, D.P., Gill, B.C., Gordon, G.W., Knoll, A.H., Nielsen, A.T., Schovsbo, N.H., and Canfield, D.E., 2010, Devonian rise in atmospheric oxygen correlated to the radiations of terrestrial plants and large predatory fish: Proceedings of the National Academy of Sciences of the United States of America, v. 107, p. 17,911–17,915, https://doi.org/10.1073/pnas.1011287107.

Day, J., Uyeno, T., Norris, W., Witzke, B.J., and Bunker, B.J., 1996, Middle-Upper Devonian relative sea-level histories of central and western North American interior basins, *in* Witzke, B.J., Ludvigson, G.A., and Day, J., eds., Paleozoic Sequence Stratigraphy; Views from the North American Craton: Geological Society of America Special Paper 306, p. 259–275, https://doi.org/10.1130/0-8137-2306-X.259.

Deland, C., and Shaw, A., 1956, Upper Cambrian trilobites from Western Wyoming: Journal of Paleontology, v. 30, no. 3, p. 542–562.

di Pasquo, M., Grader, G.W., Warren, A, Rice, B., Isaacson, P., and Doughty, P.T., 2017, Palynologic delineation of the Devonian–Carboniferous boundary, West-Central Montana, USA: Palynology, v. 41, p. 189–220, https://doi.org/10.1080/01916122.2017.1366180.

di Pasquo, M., Grader, G.W., Kondas, M., Doughty, P.T., Filipiak, P., Rice, B.J., and Isaacson, P.E., 2019, Lower Sappington Formation palynofacies in Montana confirm upper Famennian black shale paleoenvironments and sequences across western North America: Palaeogeography, Palaeoclimatology, Palaeoecology, v. 536, https://doi.org/10.1016/j.palaeo.2019.109370.

di Pasquo, M., Hu, M., Zatoń, M., and Myrow, P., 2022, Microspores, megaspores, palynofacies, and depositional history of the upper Givetian Maywood Formation, Northern Wyoming, USA: Review of Palaeobotany and Palynology, v. 299, https://doi.org/10.1016/j.revpalbo.2022.104604.

Dorf, E., 1934, Stratigraphy and paleontology of a new Devonian Formation at Beartooth Butte, Wyoming: The Journal of Geology, v. 42, no. 7, p. 720–737, https://doi.org/10.1086/624237.

Dorobek, S.L., Reid, S.K., and Elrick, M., 1991, Antler foreland stratigraphy of Montana and Idaho: The stratigraphic record of eustatic fluctuations and episodic tectonic events, *in* Cooper, J.D., and Stevens C.H., eds., Paleozoic Paleogeography of the Western United States II: Pacific Section, Stratigraphic Evolution of Foreland Basins, v. 67, no. 1, p. 487–507.

Elliott, D.K., and Ilyes, R.R., 1996, Lower Devonian vertebrate biostratigraphy of the western United States: Modern Geology, v. 20, p. 253–262.

Elliott, D.K., and Johnson, H.G., 1997, Use of vertebrates to solve biostratigraphic problems: Examples from the Lower and Middle Devonian of western North America, *in* Klapper, G., Murphy, M.A., and Talent, J.A., eds., Paleozoic Sequence Stratigraphy, Biostratigraphy, and Biogeography: Studies in Honor of J. Granville ("Jess"): Geological Society of America Special Paper 321, p. 179–188, https://doi.org/10.1130/0-8137-2321-3.179.

Falcon-Lang, H.J., and Bashforth, A.R., 2004, Pennsylvanian uplands were forested by giant cordaitalean trees: Geology, v. 32, p. 417–420, https://doi.org/10.1130/G20371.1.

Fischer, W.W., 2016, Breathing room for early animals: Proceedings of the National Academy of Sciences of the United States of America, v. 113, p. 1686–1688, https://doi.org/10.1073/pnas.1525100113.

Fischer, W.W., and Valentine, J.S., 2019, How did life come to tolerate and thrive in an oxygenated world?: Free Radical Biology & Medicine, v. 140, p. 1–3, https://doi.org/10.1016/j.freeradbiomed.2019.07.021.

Flament, N., Gurnis, M., and Müller, R.D., 2013, A review of observations and models of dynamic topography: Lithosphere, v. 5, p. 189–210, https://doi.org/10.1130/L245.1.

Foster, G.L., Royer, D.L., and Lunt, D.J., 2017, Future climate forcing potentially without precedent in the last 420 million years: Nature Communications, v. 8, p. 1–8, https://doi.org/10.1038/ncomms14845.

Foster, N.H., 1972, Ordovician system, *in* Mallory, W.W., ed., Geologic Atlas of the Rocky Mountain Region: Denver, Colorado, Rocky Mountain Association of Geologists, p. 76–85.

Gensel, P.G., and Edwards, D., 2001, Plants Invade the Land: Evolutionary and Environmental Perspectives: New York, Columbia University Press, 304 p., https://doi.org/10.7312/gens11160.

George, D., and Blieck, A., 2011, Rise of the earliest tetrapods: An Early Devonian origin from marine environment: PLoS One, v. 6, p. 1–7, https://doi.org/10.1371/journal.pone.0022136.

Girard, C., Cornée, J.-J., Joachimski, M., Charruault, A.-L., Dufour, A.-B., and Renaud, S., 2020, Paleogeographic differences in temperature, water depth and conodont biofacies during the Late Devonian: Palaeogeography, Palaeoclimatology, Palaeoecology, v. 549, no. 108852, https://doi.org/10.1016/j.palaeo.2018.06.046.

Glasspool, I.J., and Scott, A.C., 2010, Phanerozoic concentrations of atmospheric oxygen reconstructed from sedimentary charcoal: Nature Geoscience, v. 3, p. 627–630, https://doi.org/10.1038/ngeo923.

Glasspool, I.J., Edwards, D., and Axe, L., 2004, Charcoal in the Silurian as evidence for the earliest wildfire: Geology, v. 32, p. 381–383, https://doi.org/10.1130/G20363.1.

Glasspool, I.J., Scott, A.C., Waltham, D., Pronina, N., and Shao, L., 2015, The impact of fire on the Late Paleozoic Earth system: Frontiers in Plant Science, v. 6, p. 756, https://doi.org/10.3389/fpls.2015.00756.

Goddéris, Y., Donnadieu, Y., Carretier, S., Aretz, M., Dera, G., Macouin, M., and Regard, V., 2017, Onset and ending of the late Palaeozoic ice age triggered by tectonically paced rock weathering: Nature Geoscience, v. 10, p. 382–386, https://doi.org/10.1038/ngeo2931.

González, F., 2009, Reappraisal of the organic-walled microphytoplankton genus *Maranhites*: Morphology, excystment, and speciation: Review of Palaeobotany and Palynology, v. 154, p. 6–21, https://doi.org/10.1016/j.revpalbo.2008.11.004.

Goodarzi, F., and Goodbody, Q., 1990, Nature and depositional environment of Devonian coals from western Melville Island, Arctic Canada: International Journal of Coal Geology, v. 14, p. 175–196, https://doi.org/10.1016/0166-5162(90)90002-G.

Grader, G.W., and Dehler, C.M., 1999, Devonian stratigraphy in east-central Idaho: New perspectives from the Lemhi Range and Bayhorse area, *in* Hughes, S.S., and Thackray, G.D., eds., Guidebook to the Geology of Eastern Idaho: Pocatello, Idaho, USA, Idaho Museum of Natural History, p. 29–54.

Grader, G.W., Isaacson, P.E., Doughty, P.T., Pope, M.C., and Desantis, M.K., 2017, Idaho Lost River shelf to Montana craton: North American Late Devonian stratigraphy, surfaces, and intrashelf basin, *in* Playton, T.E., Kerans, C., and Weissenbergrer, J.A.W., eds., New Advances in Devonian Carbonates: Outcrop Analogs, Reservoirs and Chronostratigraphy: Society for Sedimentary Geology, v. 107, https://doi.org/10.2110/sepmsp.107.12.

Grahn, Y., and Paris, F., 2011, Emergence, biodiversification and extinction of the chitinozoan group: Geological Magazine, v. 148, p. 226–236, https://doi.org/10.1017/S001675681000052X.

Gurnis, M., 1993, Phanerozoic marine inundation of continents driven by dynamic topography above subducting slabs: Nature, v. 364, p. 589–593, https://doi.org/10.1038/364589a0.

Harland, W.B., Pickton, C.A.G., Wright, N.J.R., Croxton, C.A., Smith, D.G., Cutbill, J.L., and Henderson, W.G., 1976, Some coal-bearing strata in Svalbard: Skrifter-Norsk Polarinstitutt, v. 164, p. 7–23.

Heal, S., and Clayton, G., 2008, The palynology of the Hannibal Shale (Mississippian) of northeastern Missouri, U.S.A. and correlation with Western Europe: Palynology, v. 32, p. 27–37, https://doi.org/10.2113/gspalynol.32.1.27.

Hladil, J., Koptíková, L., Galle, A., Sedláček, V., Pruner, P., Schnabl, P., Langrová, A., Bábek, O., Frána, J., Hladíková, J., Otava, J., and Geršl, M., 2009, Early Middle Frasnian platform reef strata in the Moravian Karst interpreted as recording the atmospheric dust changes: The key to understanding perturbations in the punctate conodont zone: Bulletin of Geosciences, v. 84, p. 75–106, https://doi.org/10.3140/bull.geosci.1113.

Hofmann, M.H., 2020, The Devonian sedimentary record of Montana, *in* Barth, S., ed., Geology of Montana: Montana Bureau of Mines and Geology Special Publication 122, 51 p.

Hogancamp, N.J., and Pocknall, D.T., 2018, The biostratigraphy of the Bakken Formation: A review and new data: Stratigraphy, v. 15, p. 197–224, https://doi.org/10.29041/strat.15.3.197-224.

Holland, S.M., and Patzkowsky, M.E., 2009, The stratigraphic distribution of fossils in a tropical carbonate succession: Ordovician Bighorn Dolomite, Wyoming, USA: PALAIOS, v. 24, no. 5–6, p. 303–317.

Holmden, C., Braun, W.K., Patterson, W.P., Eglington, B.M., Prokopiuk, T.C., and Whittaker, S., 2006, Carbon isotope chemostratigraphy of Frasnian sequences in western Canada, *in* Summary of Investigations 2006, Volume 1: Regina, Saskatchewan, Canada, Saskatchewan Geological Survey, Saskatchewan Industry Resources, Misc. Rep. 2006-4.1, CD-ROM, Paper A-8, 6 p.

Huang, C., Joachimski, M.M., and Gong, Y., 2018, Did climate changes trigger the Late Devonian Kellwasser Crisis?: Evidence from a high-resolution conodont $\delta^{18}O_{PO4}$ record from South China: Earth and Planetary Science Letters, v. 495, p. 174–184.

Joachimski, M.M., van Geldern, R., Breisig, S., Day, J., and Buggisch, W., 2004, Oxygen isotope evolution of biogenic calcite and apatite during the Middle and Upper Devonian: International Journal of Earth Sciences: Geologische Rundschau, v. 93, p. 542–553.

Johnson, J.G., and Pendergast, A., 1981, Timing and mode of emplacement of the Roberts Mountains allochthon, Antler orogeny: Geological Society of America Bulletin, v. 92, p. 648–658, https://doi.org/10.1130/0016-7606(1981)92<648:TAMOEO>2.0.CO;2.

Johnson, J.G., and Sandberg, C.A., 1988, Devonian eustatic events in the western United States and their biostratigraphic responses, *in* McMillan, N.J., Embry, A.F., and Glass, D.J., eds., Devonian of the World: Canadian Society of Petroleum Geologists Memoir 14, p. 171–179.

Johnson, J.G., Klapper, G., and Sandberg, C.A., 1985, Devonian eustatic fluctuations in Euramerica: Geological Society of America Bulletin, v. 96, p. 567–587, https://doi.org/10.1130/0016-7606(1985)96<567:DEFIE>2.0.CO;2.

Kabanov, P., 2021, Early–Middle Devonian paleosols and palustrine beds of NW Canada in the context of land plant evolution and global spreads of anoxia: Global and Planetary Change, v. 204, https://doi.org/10.1016/j.gloplacha.2021.103573.

Kammer, T.W., and Matchen, D.L., 2008, Evidence for eustasy at the Kinderhookian–Osagean (Mississippian) boundary in the United States: Response to late Tournaisian glaciation?, *in* Fielding, C.R., Frank, T.D., and Isbell, J.L., eds., Resolving the Late Paleozoic Ice Age in Time and Space: Geological Society of America Special Paper 441, p. 261–274, https://doi.org/10.1130/2008.2441(18).

Katz, D.A., Buoniconti, M.R., Montañez, I.P., Swart, P.K., Eberli, G.P., and Smith, L.B., 2007, Timing and local perturbations to the carbon pool in the lower Mississippian Madison Limestone, Montana and Wyoming: Palaeogeography, Palaeoclimatology, Palaeoecology, v. 256, p. 231–253, https://doi.org/10.1016/j.palaeo.2007.02.048.

Kauffman, M.E., and Earll, F.N., 1963, Geology of the Garnet-Bearmouth Area, Western Montana: Montana Bureau of Mines and Geology Memoir M-39, 40 p.

Keefer, W.R., and Van Lieu, J.A., 1966, Paleozoic formations in the Wind River Basin, Wyoming: U.S. Geological Survey Professional Paper 495-B, 60 p., https://doi.org/10.3133/pp495B.

Kellogg, K.S., and Williams, V.S., compilers, 2000, Geologic map of the Ennis 30′ × 60′ quadrangle, Madison and Gallatin Counties, Montana, and Park County, Wyoming: U.S. Geological Survey IMAP 2690, scale 1:100,000, 16 p., https://doi.org/10.3133/i2690.

Kennedy, K.L., Gibling, M.R., Eble, C.F., Gastaldo, R.A., Gensel, P.G., Werner-Zwanziger, U., and Wilson, R.A., 2013, Lower Devonian coaly shales of northern New Brunswick, Canada: Plant accumulations in the early stages of terrestrial colonization: Journal of Sedimentary Research, v. 83, p. 1202–1215, https://doi.org/10.2110/jsr.2013.86.

Kenrick, P., and Crane, P.R., 1997, The origin and early evolution of plants on land: Nature, v. 389, p. 33–39, https://doi.org/10.1038/37918.

Kervin, R.J., and Woods, A.D., 2012, Origin and evolution of paleokarst within the Lower Ordovician (Ibexian) Goodwin Formation (Pogonip Group): Journal of Palaeogeography, v. 1, p. 57–69.

Ketner, K.B., 2012, An alternative hypothesis for the mid-Paleozoic Antler orogeny in Nevada: U.S. Geological Survey Professional Paper 1790, 11 p., https://doi.org/10.3133/pp1790.

Klapper, G., 1977, *Polygnathus linguiformis linguiformis* Hinde alpha morphotype Bultynck; *Polygnathus serotinus* Telford, *in* Ziegler, W., ed., Catalogue of Conodonts, III: Stuttgart, Germany, E. Schweizerbart'sche Verlagsbuchhandlung, p. 462, 492, 495–496.

Klug, C., Kröger, B., Kiessling, W., Mullins, G.L., Servais, T., Frýda, J., Korn, D., and Turner, S., 2010, The Devonian nekton revolution: Lethaia, v. 43, p. 465–477, https://doi.org/10.1111/j.1502-3931.2009.00206.x.

Kroeck, D.M., Mullins, G., Zacaï, A., Monnet, C., and Servais, T., 2022, A review of Paleozoic phytoplankton biodiversity: Driver for major evolutionary events?: Earth-Science Reviews, https://doi.org/10.1016/j.earscirev.2022.104113.

Kump, L.R., and Arthur, M.A., 1999, Interpreting carbon-isotope excursions: Carbonates and organic matter: Chemical Geology, v. 161, p. 181–198, https://doi.org/10.1016/S0009-2541(99)00086-8.

LaMaskin, T.A., and Elrick, M., 1997, Sequence stratigraphy of the Middle to Upper Devonian Guilmette Formation, southern Egan and Schell Creek ranges, Nevada, *in* Klapper, G., Murphy, M.A., and Talent, J.A., eds., Paleozoic Sequence Stratigraphy, Biostratigraphy, and Biogeography: Studies in Honor of J. Granville ("Jess") Johnson: Geological Society of America Special Paper 321, p. 89–112, https://doi.org/10.1130/0-8137-2321-3.89.

Lapo, A.V., and Drozdova, I.N., 1989, Phyterals of humic coals in the U.S.S.R: International Journal of Coal Geology, v. 12, p. 477–510, https://doi.org/10.1016/0166-5162(89)90062-1.

Lash, G.G., 2019, A global biogeochemical perturbation during the Middle Frasnian *punctata* Event: Evidence from muted carbon isotope signature in the Appalachian Basin, New York State (USA): Global and Planetary Change, v. 177, p. 239–254, https://doi.org/10.1016/j.gloplacha.2019.01.006.

Le Hir, G., Donnadieu, Y., Goddéris, Y., Meyer-Berthaud, B., Ramstein, G., and Blakey, R.C., 2011, The climate change caused by the land plant invasion in the Devonian: Earth and Planetary Science Letters, v. 310, p. 203–212, https://doi.org/10.1016/j.epsl.2011.08.042.

Lenton, T.M., Dahl, T.W., Daines, S.J., Mills, B.J., Ozaki, K., Saltzman, M.R., and Porada, P., 2016, Earliest land plants created modern levels of atmospheric oxygen: Proceedings of the National Academy of Sciences of the United States of America, v. 113, p. 9704–9709, https://doi.org/10.1073/pnas.1604787113.

Li, W., Xu, H., Gao, S., Yu, Y., Ning, C., Yang, J., and Jiang, T., 2021, Inner architectural characteristics of wave-dominated shoreface deposits and their geological implications: A case study of Devonian 'Donghe sandstones' in Tarim Basin, China: Marine and Petroleum Geology, v. 134, https://doi.org/10.1016/j.marpetgeo.2021.105334.

Liu, J., Algeo, T.J., Qie, W., and Saltzman, M.R., 2019, Intensified oceanic circulation during Early Carboniferous cooling events: Palaeogeography, Palaeoclimatology, Palaeoecology, v. 531, p. 108962, https://doi.org/10.1016/j.palaeo.2018.10.021.

Loucks, R.G., 1999, Paleocave carbonate reservoirs: Origins, burial depth modifications, spatial complexity, and reservoir implications: American Association of Petroleum Geologists Bulletin, v. 83, p. 1795–1834.

Love, J.D., and Christiansen, A.C., compilers, 1983, Preliminary geologic map of Wyoming: U.S. Geological Survey Open-File Report 83-802, scale 1:50,0000, https://doi.org/10.3133/ofr83802.

Lu, M., Ikejiri, T., and Lu, Y., 2021, A synthesis of the Devonian wildfire record: Implications for paleogeography, fossil flora, and paleoclimate: Palaeogeography, Palaeoclimatology, Palaeoecology, v. 571, https://doi.org/10.1016/j.palaeo.2021.110321.

Macke, D.L., 1993, Cambrian through Mississippian rocks of the Powder River Basin, Wyoming, Montana, and adjacent areas, *in* Stoeser J., ed., Evolution of Sedimentary Basins—Powder River Basin: U.S. Geological Survey Bulletin, v. 1917-M, 174 p.

Madsen, O.S., Poon, Y.K., and Graber, H.C., 1988, Spectral wave attenuation by bottom friction: Theory, *in* Proceedings of 21st International Conference on Coastal Engineering, American Society of Civil Engineering, New York, p. 492–504.

Maharjan, D., Jiang, G., Peng, Y., and Henry, R.A., 2018a, Paired carbonate-organic carbon and nitrogen isotope variations in Lower Mississippian strata of the southern Great Basin, western United States: Palaeogeography, Palaeoclimatology, Palaeoecology, v. 490, p. 462–472, https://doi.org/10.1016/j.palaeo.2017.11.026.

Maharjan, D., Jiang, G.Q., Peng, Y.B., and Nicholla, M.J., 2018b, Sulfur isotope change across the Early Mississippian K-O (Kinderhookian–Osagean) δ^{13}C excursion: Earth and Planetary Science Letters, v. 494, p. 202–215, https://doi.org/10.1016/j.epsl.2018.04.043.

Marshall, J.E.A., Brown, J.F., and Astin, T.R., 2011, Recognising the Taghanic Crisis in the Devonian terrestrial environment and its implications for understanding land-sea interactions: Palaeogeography, Palaeoclimatology, Palaeoecology, v. 304, p. 165–183, https://doi.org/10.1016/j.palaeo.2010.10.016.

Marshall, J.E.A., Holterhoff, P.F., El-Abdallah, S.R., Matsunaga, K.S., Bronson, A.W., and Tomescu, A.M.F., 2022, The Archaeopterid forests of Lower Frasnian (Upper Devonian) westernmost Laurentia: Biota and depositional environment of the Maywood Formation in northern Wyoming as reflected by palynoflora, macroflora, fauna, and sedimentology: International Journal of Plant Sciences, v. 183, p. 465–492, https://doi.org/10.1086/720736.

McGhee, G., Sheehan, P., Bottjer, D., and Droser, M., 2004, Ecological ranking of Phanerozoic biodiversity crises: Ecological and taxonomic severities are decoupled: Palaeogeography, Palaeoclimatology, Palaeoecology, v. 211, p. 289–297, https://doi.org/10.1016/j.palaeo.2004.05.010.

McNestry, A., 1988, Palynostratigraphy of two uppermost Devonian-lower Carboniferous borehole sections in South Wales: Review of Palaeobotany and Palynology, v. 56, p. 69–87, https://doi.org/10.1016/0034-6667(88)90075-9.

Meyer-Berthaud, B., Soria, A., and Decombeix, A.L., 2010, The land plant cover in the Devonian: A reassessment of the evolution of the tree habit, *in* Vecoli, M., Meyer-Berthaud, B., and Clément, G., eds., The Terrestrialization Process: Modelling Complex Interactions at the Biosphere-Geosphere Interface: Geological Society, London, Special Publication 339, p. 59–70, https://doi.org/10.1144/SP339.6.

Mii, H., Grossman, E.L., and Yancey, T.E., 1999, Carboniferous isotope stratigraphies of North America: Implications for Carboniferous paleoceanography and Mississippian glaciation: Geological Society of America Bulletin, v. 111, p. 960–973, https://doi.org/10.1130/0016-7606(1999)111<0960:CISONA>2.3.CO;2.

Morrow, J.R., Sandberg, C.A., and Harris, A.G., 2005, Late Devonian Alamo Impact, southern Nevada, USA: Evidence of size, marine site, and widespread effects, *in* Kenkmann, T., Hörz, F., and Deutsch, A., eds., Large Meteorite Impacts III: Geological Society of America Special Paper 384, p. 259–280, https://doi.org/10.1130/0-8137-2384-1.259.

Morrow, J.R., Sandberg, C.A., Malkowski, K., and Joachimski, M., 2009, Carbon isotope chemostratigraphy and precise dating of Middle Frasnian (Lower Upper Devonian) Alamo Breccia, Nevada, USA: Palaeogeography, Palaeoclimatology, Palaeoecology, v. 282, p. 105–118, https://doi.org/10.1016/j.palaeo.2009.08.016.

Mullins, G.L., and Servais, T., 2008, The diversity of the Carboniferous phytoplankton: Review of Palaeobotany and Palynology, v. 149, p. 29–49, https://doi.org/10.1016/j.revpalbo.2007.10.002.

Nawrocki, J., Polechońska, O., and Werner, T., 2008, Magnetic susceptibility and selected geochemical–mineralogical data as proxies for Early to Middle Frasnian (Late Devonian) carbonate depositional settings in the Holy Cross Mountains, southern Poland: Palaeogeography, Palaeoclimatology, Palaeoecology, v. 269, p. 176–188, https://doi.org/10.1016/j.palaeo.2008.04.032.

Olsen, T.R., Mellere, D., and Olsen, T., 1999, Facies architecture and geometry of landward-stepping shoreface tongues: The Upper Cretaceous Cliff House Sandstone (Mancos Canyon, south-west Colorado): Sedimentology, v. 46, p. 603–625, https://doi.org/10.1046/j.1365-3091.1999.00234.x.

Peterson, J.A., 1981, Stratigraphy and sedimentary facies of the Madison limestone and associated rocks in parts of Montana, North Dakota, South Dakota, Wyoming, and Nebraska: U.S. Geological Survey Numbered Series 81-642, 92 p.

Pisarzowska, A., and Racki, G., 2012, Isotopic geochemistry across the Early–Middle Frasnian transition (Late Devonian) on the South Polish carbonate shelf: A reference for the global *punctata* event: Chemical Geology, v. 334, p. 199–220, https://doi.org/10.1016/j.chemgeo.2012.10.034.

Pisarzowska, A., and Racki, G., 2020, Comparative carbon isotope chemostratigraphy of major Late Devonian biotic crises: Stratigraphy & Timescales, v. 5, p. 387–466, https://doi.org/10.1016/bs.sats.2020.08.001.

Pisarzowska, A., Sobstel, M., and Racki, G., 2006, Conodont-based event stratigraphy of the Early–Middle Frasnian transition on South Polish carbonate shelf: Acta Palaeontologica Polonica, v. 51, p. 609–646.

Pisarzowska, A., Becker, R., Aboussalam, Z., Marek, S., Sobień, K., Kremer, B., Owocki, K., and Racki, G., 2020, Middlesex/*punctata* Event in the Rhenish Basin (Padberg section, Sauerland, Germany): Geochemical clues to the early-middle Frasnian perturbation of global carbon cycle: Global and Planetary Change, v. 191, p. 1–14, https://doi.org/10.1016/j.gloplacha.2020.103211.

Qiao, L., and Shen, S.Z., 2014, Global paleobiogeography of brachiopods during the Mississippian—Response to the global tectonic reconfiguration, ocean circulation, and climate changes: Gondwana Research, v. 26, p. 1173–1185, https://doi.org/10.1016/j.gr.2013.09.013.

Qie, W., Algeo, T.J., Luo, G., and Herrmann, A., 2019, Global events of the Late Paleozoic (Early Devonian to Middle Permian): A review: Palaeogeography, Palaeoclimatology, Palaeoecology, v. 531, p. 1–15, https://doi.org/10.1016/j.palaeo.2019.109259.

Qie, W.K., Zhang, X.H., Du, Y.S., and Zhang, Y., 2011, Lower Carboniferous carbon isotope stratigraphy in South China: Implications for the Late Paleozoic glaciation: Science China: Earth Sciences, v. 54, p. 84–92, https://doi.org/10.1007/s11430-010-4062-4.

Racki, G., 2020, Volcanism as a prime cause of mass extinction: Retrospectives and perspectives, *in* Adatte, T., Bond, D.P.G., and Keller, G., eds., Mass Extinctions, Volcanism, and Impacts: New Developments: Geological Society of America Special Paper 544, p. 1–34, https://doi.org/10.1130/2020.2544(01).

Racki, G., Joachimski, M.M., and Morrow, J.R., 2008, A major perturbation of the global carbon budget in the Early–Middle Frasnian transition (Late Devonian): Palaeogeography, Palaeoclimatology, Palaeoecology, v. 269, p. 127–129, https://doi.org/10.1016/j.palaeo.2008.04.030.

Riegel, W., 2008, The Late Palaeozoic phytoplankton blackout: Artefact or evidence of global change?: Review of Palaeobotany and Palynology, v. 148, p. 73–90, https://doi.org/10.1016/j.revpalbo.2006.12.006.

Saltzman, M.R., 2002, Carbon isotope $\delta^{13}C$ stratigraphy across the Silurian–Devonian transition in North America: Evidence for a perturbation of the global carbon cycle: Palaeogeography, Palaeoclimatology, Palaeoecology, v. 187, p. 83–100, https://doi.org/10.1016/S0031-0182(02)00510-2.

Saltzman, M.R., 2003, Organic carbon burial and phosphogenesis in the Antler foreland basin: An out-of-phase relationship during the lower Mississippian: Journal of Sedimentary Research, v. 73, p. 844–855, https://doi.org/10.1306/032403730844.

Sandberg, C.A., 1961a, Distribution and thickness of Devonian rocks in Williston basin and in central Montana and north-central Wyoming: U.S. Geological Survey Bulletin, v. 1112-D, p. 105–127.

Sandberg, C.A., 1961b, Widespread Beartooth Butte Formation of Early Devonian age in Montana and Wyoming and its paleogeographic significance: American Association of Petroleum Geologists Bulletin, v. 45, p. 1301–1309, https://doi.org/10.1306/BC7436E1-16BE-11D7-8645000102C1865D.

Sandberg, C.A., 1963, Spirorbal Limestone in the Souris River(?) Formation of Late Devonian age at Cottonwood Canyon, Bighorn Mountains, Wyoming: U.S. Geological Survey Professional Paper 475-C, p. 14–16.

Sandberg, C.A., 1965, Nomenclature and correlation of lithologic subdivisions of the Jefferson and Three Forks formations of southern Montana and northern Wyoming: Geological Survey Bulletin, v. 1194-N, 18 p.

Sandberg, C.A., and Klapper, G., 1967, Stratigraphy, age, and paleotectonic significance of the Cottonwood Canyon Member of the Madison Limestone in Wyoming and Montana: Geological Survey Bulletin, v 1251-B, 70 p.

Sandberg, C.A., and McMannis, W.J., 1964, Occurrence and paleogeographic significance of the Maywood Formation of Late Devonian age in the Gallatin range, southwestern Montana: U.S. Geological Survey Professional Paper 501-C, p. 50–54.

Sandberg, C.A., and Poole, F.G., 1977, Conodont biostratigraphy and depositional complexes of Upper Devonian cratonic platform and continental-shelf rocks in the Western United States, in Murphy, M.A., Berry, W.B.N., and Sandberg, C.A., eds., Western North America: Devonian: Riverside, California, USA, University of California Museum Contribution, v. 4, p. 144–182.

Sandberg, C.A., Poole, F.G., and Johnson, J.G., 1988, Upper Devonian of western United States, in McMillan, N.J., Embry, A.F., and Glass, D.J., eds., Devonian of the World, Volume III: Canadian Society of Petroleum Geologists Memoir v. 14, p. 183–220.

Sandberg, C.A., Morrow, J.R., and Warme, J., 1997, Late Devonian Alamo impact event, global Kellwasser events, and major eustatic events, eastern Great Basin, Nevada and Utah: Geology Studies, v. 42, p. 129–160.

Sandberg, C.A., Morrow, J.R., and Ziegler, W., 2002, Late Devonian sea-level changes, catastrophic events, and mass extinctions, in Koeberl, C., and MacLeod, K.G., eds., Catastrophic Events and Mass Extinctions: Impacts and Beyond: Geological Society of America Special Paper 356, p. 473–487, https://doi.org/10.1130/0-8137-2356-6.473.

Sarjeant, W.A.S., and Stancliffe, R.P.W., 1994, The *Michrystridium* and *Veryhachium* complexes (Acritarcha: Acanthomorphitae and Polygonomorphitae): A taxonomic reconsideration: Micropaleontology, v. 40, p. 1–77, https://doi.org/10.2307/1485800.

Scheckler, S.E., 2001, Afforestation—The first forests, in Briggs, D.E.G., and Crowther, P., eds., Palaeobiology II: Oxford, UK, Blackwell, p. 67–71, https://doi.org/10.1002/9780470999295.ch13.

Scott, A.C., and Glasspool, I.J., 2006, The diversification of Palaeozoic fire systems and fluctuations in atmospheric oxygen concentration: Proceedings of the National Academy of Sciences of the United States of America, v. 103, p. 10,861–10,865, https://doi.org/10.1073/pnas.0604090103.

Scott, A.C., Bowman, D.M.J.S., Bond, W.J., Pyne, S.J., and Alexander, M.E., 2013, Fire On Earth: An Introduction: Hoboken, New Jersey, USA, Wiley-Blackwell, 434 p.

Shinn, E.A., 1983, Birdseyes, fenestrae, shrinkage pores, and loferites: A reevaluation: Journal of Sedimentary Research, v. 53, p. 619–628, https://doi.org/10.1306/212F8247-2B24-11D7-8648000102C1865D.

Signor, P.W.I.I.I., and Brett, C.E., 1984, The mid-Paleozoic precursor to the Mesozoic marine revolution: Paleobiology, v. 10, p. 229–245, https://doi.org/10.1017/S0094837300008174.

Silberling, N.J., and Roberts, R.J., 1962, Pre-Tertiary Stratigraphy and Structure of Northwestern Nevada: Geological Society of America Special Paper 72, 56 p., https://doi.org/10.1130/SPE72-p1.

Śliwiński, M., Whalen, M., Newberry, R., Payne, J., and Day, J., 2011, Stable isotope ($\delta^{13}C_{carb\ and\ org}$, $\delta^{15}N_{org}$) and trace element anomalies during the Late Devonian '*punctata* Event' in the western Canada Sedimentary Basin: Palaeogeography, Palaeoclimatology, Palaeoecology, v. 307, p. 245–271, https://doi.org/10.1016/j.palaeo.2011.05.024.

Smith, J.F., Jr., and Ketner, K.B., 1968, Devonian and Mississippian rocks and the date of the Roberts Mountains thrust in the Carlin-Piñon Range area, Nevada: U.S. Geological Survey Bulletin, v. 1251-I, 18 p.

Speed, R.C., Elison, M.W., and Heck, F.R., 1988, Phanerozoic tectonic evolution of the Great Basin, in Ernst, W.G., ed., Metamorphism and crustal evolution of the western United States (Rubey Volume VII): Englewood Cliffs, New Jersey, USA, Prentice-Hall, p. 572–605.

Stancliffe, R.P.W., and Sarjeant, W.A.S., 1994, The acritarch genus *Veryhachium* Deunff 1954, Emend. Sarjeant and Stancliffe 1994: A taxonomic restudy and reassessment of its constituent species: Micropaleontology, v. 40, p. 223–241, https://doi.org/10.2307/1485817.

Stancliffe, R.P.W., and Sarjeant, W.A.S., 1996, The acritarch genus *Dorsennidium* Wicander 1974, Emend. Sarjeant and Stancliffe 1994: A reassessment of its constituent species: Micropaleontology, v. 42, p. 151–166, https://doi.org/10.2307/1485867.

Stein, W.E., Berry, C.M., Morris, J.L., Hernick, L.V., Mannolini, F., Ver Straeten, C., Landing, E., Marshall, J.E.A., Wellman, C.H., Beerling, D.J., and Leaket, J.R., 2020, Mid-Devonian *Archaeopteris* roots signal revolutionary change in earliest fossil forests: Current Biology, v. 30, p. 421–431, https://doi.org/10.1016/j.cub.2019.11.067.

Stewart, W.N., and Rothwell, G.W., 1993, Paleobiology and the evolution of plants: Cambridge, UK, Cambridge University Press, 521 p.

Streel, M., 1999, Quantitative palynology of Famennian events in the Ardenne-Rhine regions, in Feist, R., Talent, J.A., and Daurer, A., eds., North Gondwana: Mid-Paleozoic Terranes, Stratigraphy and Biota: Abhandlungen der Geologischen Bundesanstalt, v. 54, p. 201–212.

Streel, M., Boulvain, F., Dusar, M., Loboziak, S., and Steemans, P., 2021, Updating Frasnian miospore zonation from the Boulonnais (Northern France) and comparison with new data from the Upper Palaeozoic cover on the Brabant Massif (Western Belgium): Geologica Belgica, v. 24, p. 69–84, https://doi.org/10.20341/gb.2020.024.

Tanner, W., 1984, A fossil flora from the Beartooth Butte Formation of northern Wyoming [Ph.D. dissertation]: Carbondale, Illinois, USA, Southern Illinois University, 222 p.

Tappan, H., 1980, The Paleobiology of Plant Protists: San Francisco, California, USA, W.H. Freeman, 1028 p.

Tucker, M.E., and Wright, V.P., 1990, Chapter 4.3: Peritidal carbonates, in Tucker, M.E., and Wright V.P., eds., Carbonate Sedimentology: Hoboken, New Jersey, USA, Wiley-Blackwell, p. 137–164, https://doi.org/10.1002/9781444314175.

Turnau, E., 2011, Palinostratigrafia dewonu obszaru radomsko-lubelskiego, in Narkiewicz, M., ed., Baseny Dewońskie Południowo-Wschodniej Polski: Warszawa, Poland, Prace Państwowego Instytutu Geologicznego, Państwowy Instytut Geologiczny Państwowy Instytut Badawczy, v. 196, p. 255–276.

Turnau, E., 2014, Floral change during the Taghanic Crisis: Spore data from the Middle Devonian of northern and south-eastern Poland: Review of Palaeobotany and Palynology, v. 200, p. 108–121, https://doi.org/10.1016/j.revpalbo.2013.08.004.

Turnau, E., and Racki, G., 1999, Givetian palynostratigraphy and palynofacies: New data from the Bodzentyn Syncline (Holy Cross Mountains, central Poland): Review of Palaeobotany and Palynology, v. 106, p. 237–271, https://doi.org/10.1016/S0034-6667(99)00011-1.

Volkova, I.B., 1994, Nature and composition of the Devonian coals of Russia: Energy & Fuels, v. 8, p. 1489–1493, https://doi.org/10.1021/ef00048a039.

Veevers, J.J., and Powell, M., 1987, Late Paleozoic glacial episodes in Gondwanaland reflected in transgressive–regressive depositional sequences in Euramerica: Geological Society of America Bulletin, v. 98, p. 475–487, https://doi.org/10.1130/0016-7606(1987)98<475:LPGEIG>2.0.CO;2.

Vuke, S.M., Lonn, J.D., Berg, R.B., and Schmidt, C.J., compilers, 2014, Geologic map of the Bozeman 30′ × 60′ quadrangle southwestern Montana: Montana Bureau of Mines and Geology Open-File Report 648, 44 p.

Wallace, M.W., Shuster, A., Greig, A., Planavsky, N.J., and Reed, C.P., 2017, Oxygenation history of the Neoproterozoic to early Phanerozoic and the rise of land plants: Earth and Planetary Science Letters, v. 466, p. 12–19, https://doi.org/10.1016/j.epsl.2017.02.046.

Warme, J.E., and Sandberg, C.A., 1995, The catastrophic Alamo breccia of southern Nevada, Record of a Late Devonian extraterrestrial impact: Courier Forschungsinstitut Senckenberg, v. 188, no. 3137.

Watson, A.J., and Lovelock, J.E., 2013, The dependence of flame spread and probability of ignition on atmospheric oxygen, in Belcher, C.M., ed., Fire Phenomena and the Earth System: An Interdisciplinary Guide to Fire Science: Chichester, UK, John Wiley and Sons, p. 273–287, https://doi.org/10.1002/9781118529539.ch14.

Wesolowski, L.J., Buatois, L.A., Mángano, M.G., Ponce, J.J., and Carmona, N.B., 2018, Trace fossils, sedimentary facies and parasequence architecture from the Lower Cretaceous Mulichinco Formation of Argentina: The role of fair-weather waves in shoreface deposits: Sedimentary Geology, v. 367, p. 146–163, https://doi.org/10.1016/j.sedgeo.2018.02.007.

Wicander, R., and Playford, G., 2013, Marine and terrestrial palynofloras from transitional Devonian–Mississippian strata, Illinois Basin, U.S.A.: Boletín Geológico y Minero, v. 124, p. 589–637.

Woodard, S.C., Thomas, D.J., Grossman, E.L., Olszewski, T.D., Yancey, T.E., Miller, B.V., and Raymond, A., 2013, Radiogenic isotope composition of Carboniferous seawater from North American epicontinental seas: Palaeogeography, Palaeoclimatology, Palaeoecology, v. 370, p. 51–63, https://doi.org/10.1016/j.palaeo.2012.11.018.

Yans, J., Corfield, R.M., Racki, G., and Preat, A., 2007, Evidence for perturbation of the carbon cycle in the Middle Frasnian *punctata* Zone (Late Devonian): Geological Magazine, v. 144, p. 263–270, https://doi.org/10.1017/S0016756806003037.

Yao, L., Qie, W., Luo, G., Liu, J., Algeo, T.J., Bai, X., Yang, B., and Wang, X., 2015, The TICE event: Perturbation of carbon-nitrogen cycles during the mid-Tournaisian (Early Carboniferous) greenhouse-icehouse transition: Chemical Geology, v. 401, p. 1–14, https://doi.org/10.1016/j.chemgeo.2015.02.021.

Zatoń, M., Vinn, O., and Tomescu, A.M.F., 2012, Invasion of freshwater and variable marginal marine habitats by microconchid tubeworms—An evolutionary perspective: Geobios, v. 45, p. 603–610, https://doi.org/10.1016/j.geobios.2011.12.003.

Zatoń, M., Hu, M., di Pasquo, M., and Myrow, P.M., 2022, Adaptive function and phylogenetic significance of novel skeletal features of a new Devonian microconchid tubeworm (Tentaculita) from Wyoming, USA: Journal of Paleontology, v. 96, p. 112–126.